Taylor & Francis
Taylor & Francis Group

Canadian Journal of Remote Sensing
Journal canadien de télédétection

ISSN: 0703-8992 (Print) 1712-7971 (Online) Journal homepage: https://www.tandfonline.com/loi/ujrs20

Integrated Object-Based Spatiotemporal Characterization of Forest Change from an Annual Time Series of Landsat Image Composites

Cristina Gómez, Joanne C. White, Michael A. Wulder & Pablo Alejandro

To cite this article: Cristina Gómez, Joanne C. White, Michael A. Wulder & Pablo Alejandro (2015) Integrated Object-Based Spatiotemporal Characterization of Forest Change from an Annual Time Series of Landsat Image Composites, Canadian Journal of Remote Sensing, 41:4, 271-292, DOI: 10.1080/07038992.2015.1089162

To link to this article: https://doi.org/10.1080/07038992.2015.1089162

Canadian Journal of Remote Sensing, 41:271–292, 2015

ISSN: 0703-8992 print / 1712-7971 online
DOI: 10.1080/07038992.2015.1089162

Taylor & Francis
Taylor & Francis Group

Integrated Object-Based Spatiotemporal Characterization of Forest Change from an Annual Time Series of Landsat Image Composites

Cristina Gómez[1*], Joanne C. White[2], Michael A. Wulder[2], and Pablo Alejandro[3]

[1]*Department of Geography and Environment, School of Geoscience, University of Aberdeen, Aberdeen AB24 3UE, Scotland, UK*
[2]*Canadian Forest Service (Pacific Forestry Centre), Natural Resources Canada, Victoria, British Columbia, V8Z 1M5, Canada*
[3]*17 Deveron Park, Huntly, AB54 8UZ, Scotland, UK*

Abstract. Identifying and mapping the location, extent, severity, and causal agent of forest change events is necessary for obtaining a wide range of information. Using 6 ecologically representative test sites (each ∼ 800 km^2) in the province of Saskatchewan, Canada, for the period 1998–2012, our objective was to prototype an object-based approach for identifying spectral change features, filling data gaps in Landsat reflectance annual best-available-pixel (BAP) composites, and attributing change processes to the derived stand-like spatial objects. The tasseled cap angle (TCA), which combines information from the visible, near-infrared, and midinfrared, enabled the description of landscape condition and its temporal derivative, the process indicator (PI), relates the rate and directionality of change at the landscape level. Data gaps, as well as anomalous values identified using time-series similarity analysis with dynamic time warping and cross-correlation measures, were replaced by spatiotemporal interpolation, resulting in annual proxy composites with no missing values. An assessment of proxy values against surface reflectance values indicated high agreement for reflectance bands (R = 0.79–0.96, RMSE = 0.005–0.021) and for TCA (R = 0.93, RMSE = 0.005), and a decrease in reliability of the proxy value as the size of the spatiotemporal gap increased, with longer temporal gaps having a greater impact on infill reliability than larger spatial gaps. Distinctive change dynamics of the sample sites were captured, demonstrating a capacity to simultaneously identify low and high magnitude changes as well as positive (e.g., growth) and negative (e.g., wildfire) trajectories using the PI. The approach presented herein provides a robust option for monitoring forest change by simultaneously describing state and ongoing change processes.

Résumé. L'identification et la cartographie de la localisation, de l'étendue, de la gravité et de l'agent causal des évènements de changements des forêts sont nécessaires pour un large éventail de besoins d'information. En utilisant 6 sites écologiquement représentatifs (d'environ 800 km^2 chacun) en Saskatchewan, au Canada, de 1998 à 2012, notre objectif était de développer une approche basée sur l'objet pour identifier les caractéristiques de changements spectraux, de combler les données manquantes dans des composites annuels de meilleur pixel disponible (BAP) de Landsat pour la réflectance, et d'attribuer les processus de changements aux objets spatiaux dérivés. Le « tasseled cap angle » (TCA), qui combine les informations du visible, du proche infrarouge et de l'infrarouge moyen, a permis la description de l'état du paysage et sa dérivée temporelle, le « process indicator » a permis la description des taux et la direction des changements au niveau du paysage. Les lacunes dans les données, ainsi que les valeurs anomales qui ont été identifiées en utilisant l'analyse de similarité de séries temporelles avec le « dynamic time warping » et les mesures d'intercorrélation, ont été remplacées par l'interpolation spatio-temporelle, qui a conduit à des composites d'estimateurs annuels sans valeurs manquantes. Une évaluation des valeurs d'estimateurs contre les valeurs de réflectance de surface a indiqué un accord élevé pour les bandes de réflectance (R = 0.79–0.96, RMSE = 0.005–0.021) et pour le TCA (R = 0.93, RMSE = 0.005), et une diminution de la fiabilité des valeurs d'estimateurs lorsque la taille de l'écart spatio-temporelle augmente. Les plus longues lacunes temporelles ayant un plus grand impact sur la fiabilité de remplissage que les lacunes spatiales plus grandes. Les dynamiques de changement distinctives des sites d'échantillonnage ont été capturées, démontrant une capacité à identifier simultanément les changements de magnitudes faibles et élevées ainsi que des trajectoires positives (par exemple, la croissance) et négatives (par exemple, feu de forêt) à l'aide du PI. L'approche présentée ici fournit une option robuste pour le suivi des changements forestiers en décrivant simultanément l'état actuel et les processus de changements.

INTRODUCTION

Change events in forest environments can be spatially and temporally discrete, such as stand replacement subsequent to wildfires or harvesting, or alternatively, change events can be

Received 24 April 2015. Accepted 7 July 2015.
*Corresponding author e-mail: c.gomez@abdn.ac.uk

spatially and temporally diffuse, resulting from forest growth, successional processes, or forest health issues (Coops et al. 2006). Sudden disturbances have an impact on the development of forest ecosystems (Oliver and Larson 1996), influencing the structure, composition, and function of forests (Franklin et al. 2002; Frolking et al. 2009), whereas subtle, slow, continuous agents of change typically have longer-term and less obvious effects on the landscape (Coops et al. 2006). Identifying and mapping the location, extent, severity, and causal agent of change events is necessary in order to obtain a wide range of information needs, including forest management (Long 2009), carbon accounting (Kurz et al. 2008, 2013; Houghton et al. 2012), biodiversity and habitat assessment (Duro et al. 2007; Berland et al. 2008), and climate change mitigation and adaptation strategies (LeQuéré et al. 2009, 2012).

Remotely sensed data provide information with inherent spatial reference that is well suited for characterizing change events in forested landscapes (Coppin et al. 2004). In particular, medium spatial resolution imagery has been demonstrated as a highly informative source of data for detection of change at human or management scales (Wulder, White, Goward, et al. 2008; Achard and Hansen 2013). Change detection approaches based on remotely sensed data are diverse (Singh 1989; Gong and Xu 2003; Coppin et al. 2004; Lu et al. 2004), differing in terms of the technique used for analysis, the spatial units considered (Hussain et al. 2013), and the amount of data required. Bitemporal change detection techniques are based on the contrast between image pairs representative of different times (e.g., Masek et al. 2008; White et al. 2011) and provide a measure of variation between instantaneous representations of the state or condition of the landscape (Kennedy et al. 2014). Bitemporal approaches require empirical or automatic selection of a threshold, derived using calibration data of some form (Xian et al. 2009). The choice and appropriateness of the time interval between pairs of images often depends on information requirements (Jensen 2005), characteristics of the change agent (Coppin and Bauer 1996), successional condition (Jin and Sader 2005), and availability of data. In contrast, change detection methods relying on a relatively dense time series of anniversary images (e.g., Huang, Goward, Masek, et al. 2009; Kennedy et al. 2010) are based on frequent observations and can provide information about trends and rates of change (Vogelmann et al. 2009) as well as successional processes (Gómez et al. 2011). With a time series approach, increasingly transient and subtle change can be identified (Kennedy et al. 2007; Brooks et al. 2013), being of particular relevance in regions of rapid recovery and growth following disturbance (Lunetta et al. 2004; Huang, Goward, Schleeweis, et al. 2009). Furthermore, the temporal features (e.g., onset and duration) of a spectral variation associated with forest change provide practical information for characterization of the magnitude and type of ongoing processes, whereas the spatial component (assuming adequate resolution) identifies the location, extent, and distribution of events. Driven by improved computing capacity, enhanced statistical algorithms, and increased availability of data, techniques continue to evolve and provide more detailed information regarding landscape change (Hansen and Loveland 2012).

Annual image time-series over forest environments enables characterization of change and change processes, integrating features such as magnitude, direction, and persistence. Further, best-available-pixel (BAP) image compositing using Landsat surface reflectance data can produce spatially exhaustive, large-area, dense time-series data conveying unique information on forest dynamics. Spatial and temporal data gaps can persist in image composites for a variety of reasons, including data availability and compositing rules. Our goal in this research is to investigate and demonstrate the capacity of a time series of annual Landsat BAP image composites for characterization of landscape-level forest change. For this purpose, we apply a multitemporal segmentation approach to generate spatial analysis units and a spectral index temporal derivative approach that enables simultaneous description of forest state and processes of change. Specific objectives of this work are to

- Fill in data gaps in series of 15 annual image composites (1998–2012) by applying a spatiotemporal interpolation algorithm;
- Characterize forest landscape change dynamics and describe ongoing processes at each date, including those that are spatially and temporally discrete as well as those that are spatially and temporally diffuse;
- Generate a series of annual proxy image composites (White et al. 2014), whereby the aforementioned change dynamics and the similarity of change processes that occur in neighboring pixels are used to detect and replace anomalous values in a pixel's temporal trajectory.

BACKGROUND

Opportunities for Improved Detection of Change

Data availability is influenced by factors such as the revisit interval of a given sensor, the presence of atmospheric instabilities (i.e., cloud, shadow, haze, smoke) over the area of interest, and the access ability (e.g., data policy, archive presence and content, historical legacy). Full access to image repositories provided by open data policies (e.g., INPE, USGS Landsat archive; Wulder et al. 2012) offers opportunities to advance processing, modelling, and data analysis techniques (Wulder and Coops 2014). Moreover, the availability of applications-ready data products with consistent radiometric and geometric properties reduces preprocessing requirements and enables automation of BAP compositing approaches that employ logical rules, such as avoidance of cloud or nonrepresentative phenological conditions. In turn, the production of high-quality image composite products enables the development of more advanced bitemporal and time-series change detection approaches, improving the reliability of results. Examples of enhanced intermediate prod-

ucts are large-area seasonal (Roy, Ju, Kline, et al. 2010), annual (Broich et al. 2011), and multiyear (Potapov et al. 2011) composites, as well as a dense time-series characterization protocol that incorporates a pixel selection and compositing phase (Kennedy et al. 2012). For identification of processes (e.g., Kennedy et al. 2010; Gómez et al. 2011) and estimation of process-derived forest structure (Pflugmacher et al. 2012; Frazier et al. 2014; Gómez et al. 2014), time series of satellite images have shown to be an increasingly reliable and informative approach.

Notwithstanding the improved accessibility to Landsat data through global archive consolidation efforts (Roy et al. 2014), the amount of good quality imagery captured over different parts of the globe is variable (Roy, Ju, Mbow, et al. 2010; White and Wulder 2013). Cloud seasonality regime, data gaps resulting from the Landsat 7 Scan Line Corrector (SLC) failure, particular policies and capacities of International Cooperator stations, and program-related image acquisition strategies are key reasons for the variation of data availability within the global Landsat archive. All Landsat imagery acquired over Canada and received by the Canadian Centre for Remote Sensing has been shared with the United States Geological Survey (USGS) through a global archive consolidation program (Wulder, White, Goward, et al. 2008); as a result, over 605,000 images are available for Canada in a calibrated and analysis-ready form (White and Wulder 2013).

Developing temporal image compositing methods to obtain wall-to-wall coverage at annual intervals is a current challenge being addressed for large area monitoring applications. Temporal composites over extensive regions (Broich et al. 2011; Griffiths, Van der Linden, et al. 2013) have demonstrated the utility of rule- and model-based processing of massive amounts of image data. Issues such as haze, smoke, residual cloud (and associated shadows) continue to be a challenge, as these features can now be reliably detected (Zhu and Woodcock 2012; Zhu et al. 2015), but they result in data gaps that require infilling if wall-to-wall image coverage is desired (e.g., Hermosilla et al. 2015). Discrete changes that occur during the growing season might also confound annual BAP composites, resulting in outcomes with suboptimal quality for certain applications, (e.g., identification of fires or silvicultural interventions; White et al. 2014). As such, new ways of processing and analysing composite images are recommended for refined product development (Griffiths, Kuemmerle, et al. 2013), as well as to deal with the apparent high levels of commission errors in maps of forest loss (Broich et al. 2011).

Filling Data Gaps

Landsat 7 ETM+ SLC-off images (captured after May 31, 2003) have ∼22 % of the image area composed of missing values (Arvidson et al. 2006). Haze, smoke, clouds and associated shadows, or other anomalous pixel values need to be removed prior to data analysis in order to avoid erroneous results and/or interpretations. The presence of data gaps in BAP annual composites over areas of frequent fire and persistent cloud regime can make it difficult to detect or attribute a given event to the correct date (Hermosilla et al. 2015). Both temporal and spatial methods for filling data gaps in Landsat imagery have been developed. Soon after the Landsat 7 ETM+ SLC failure, methods based on local linear-histogram-matching (USGS 2004), single or multilevel object-based segmentation (Maxwell 2004; Maxwell et al. 2007) and fusion with MODIS data (Roy et al. 2008) were explored. Although the application of such methods might improve the visual quality of images, the results might not provide appropriate reflectance values to support further analyses, particularly in spatially or temporally heterogeneous areas (Zhu et al. 2012). Geostatistical methods that avail on contextual proximity (Zhang et al. 2007; Pringle et al. 2009) have proven superior to deterministic methods, informing of the uncertainty in predicted values, but tend to fail with linear features and can produce striping effects (Zhu et al. 2012). In general, methods using the temporal context produce more accurate gap filling (Chen et al. 2011; Zhu et al. 2012; Zeng et al. 2013). For example, integrating temporal (intra-annual) and spatial context, Chen et al. (2011) approach (Neighborhood Similar Pixel Interpolator: NSPI) yielded accurate results in heterogeneous areas and for small or narrow landscape features. This method was augmented by Zhu et al. (2012) (Geostatistical Neighborhood Similar Pixel Interpolator: GNSPI) with geostatistical theory, specifying temporal trends by land cover type and providing uncertainty estimates. NSPI and GNSPI assume no land cover change during the period between the target and auxiliary images and require some predetermined parameters for land cover classification. Zeng et al. (2013) proposed a filling method employing multitemporal weighted linear regression, and Cheng et al. (2014) introduced a spatiotemporal Markov Random Field to identify recovering pixels, both getting accurate and improved results in heterogeneous areas, although at the cost of complex and computationally expensive methods.

Spatial Context and Temporal Information for Characterization of Landscape-Level Change

Landscape monitoring with remotely sensed data requires combined interpretation of both the spatial and temporal characteristics of the forest spectral response. Spectral variations in time and through space inform ongoing processes and spatial differences in forest cover and structure. Furthermore, processes of forest change have been shown to correlate in both space and time (Gómez et al. 2011).

Object-based techniques for image processing and data analysis facilitate incorporation of the spatial context for description of landscape change. As an alternative to pixel-based methods, groups of contiguous pixels are treated as individual entities characterized by averaged spectral values, and by contextual traits such as size, shape, internal variability, or distance to neighbors in a multidimensional feature space. Advantages of object-based methods for change detection include minimiza-

tion of registration errors and shadowing effects (Johansen et al. 2010), reduction of spectral variation for better discrimination of cover types (Costa et al. 2014), and the ability to address a multiplicity of spatial scales (Blaschke et al. 2014). The spatial resolution of imagery and the scale chosen for analysis are crucial elements in object-based change detection approaches (Chen et al. 2012; Hussain et al. 2013). A range of methods combining spatial context and temporal information have been applied for characterization of forest landscape change (Table 1). The foundations for defining meaningful objects for analysis of change include preexisting geographic information system (GIS) layers (Walter 2004), independent delineation in each image (Kindu et al. 2013), definition in a reference image for later comparison in other dates (Hall and Hay 2003), or multidate image partitioning (Desclée et al. 2006). Likewise, to avoid the uncertainty of sliver polygons, segmentation may be constrained (Li et al. 2009), hierarchical (Nijland et al. 2010), or simultaneous (Ernst et al. 2012). Multiscale image segmentation provides diverse and enhanced opportunities for analysis of change at various spatial (Duveiller et al. 2008; Vergheggen et al. 2010) and spatiotemporal scales (Gómez et al. 2011). The strengths and disadvantages identified in Table 1 may differ with variations in the classification algorithm (e.g., supervised or unsupervised) or segmentation logic (i.e., similarity criteria, hierarchy).

Defining objects that retain meaning over time is one of the biggest challenges of change detection approaches supported by spatial objects (Chen et al. 2012). Homogenous entities identified as baseline at initial stages of analysis can change partially over time, reducing object integrity (or clarity) in support of interpretation. Multitemporal segmentation, the partition of a multidate image stack (Desclée et al. 2006), ensures significance of objects on various dates by inherent definition.

Combining the strengths of multitemporal segmentation with that of time series analysis, Gómez et al. (2011) implemented a flexible method for simultaneously describing static and dynamic conditions in forest ecosystems. By means of a hierarchical spatiotemporal segmentation, a multiscale system of landscape units was defined, whereby the transition between larger and smaller objects (defined with information of initial and final condition, respectively) is driven by a time series of processes identified by a spectral index. As the term implies, spatiotemporal segmentation considers both spatial and temporal information simultaneously when objects are defined. The system of spatial units for description of the landscape state and change is purpose built, conferring the method adaptability to a variety of applications, length of analysis period, and monitoring needs. Time series of spectral data characterize the state of the landscape within analysis units at each measured time, and the temporal derivative of the spectral series enables identification of the rate and directionality of change, identifying simultaneously positive and negative changes (e.g., growth and stress) at individual dates. Application of such an approach (e.g., Gómez et al. 2011) facilitate description of both abrupt (e.g., stand-replacing harvest or fire) and subtle (e.g., insect outbreak, natural growth) processes of change, and can deal with an irregular and spare distribution of temporal data.

METHODS

Overview

A series of annual BAP composites of Landsat surface reflectance data (White et al. 2014) and derived tasseled cap angle (TCA) image composites were subject to a 3-dimensional (spatiotemporal) interpolation for generation of gap-free proxy composites and characterization of forest change dynamics. After initial infilling by spatiotemporal interpolation, objects (spatial units) were generated from spatiotemporal segmentation of the TCA image stack. These spatial units were used to evaluate the state and processes of change at the landscape level by analyzing the trajectories of the TCA and its temporal derivative (the process indicator or PI; Gómez et al. 2011). We aimed to refine the quality of the BAP composites as a source of data for other applications. With this goal, anomalies in the original annual BAP composites were detected using a similarity analysis of spectral time series and, as per data gaps, anomalous values were replaced with proxy values generated using the spatiotemporal interpolation algorithm. The final outputs of the methods applied are a spatial database providing detailed characterization of forest landscape dynamics and the proxy image composites, which represent wall-to-wall surface reflectance composites with no spatial or temporal data gaps. Figure 1 summarizes the main stages of the methods applied.

Data and Study Areas

Fifteen annual BAP composites (1998–2012) of Landsat surface reflectance data (via LEDAPS, (Masek et al. 2006; Schmidt et al. 2013)) were used in this research. The original composites incorporate Landsat TM and ETM+ images acquired during the growing season (August 1 ± 30 days) through a rule-based pixel selection process (see White et al. 2014 for details on processing and compositing methods used to generate the annual BAP composites). Six sample areas (each approximately 800 km^2 in size, Figure 2, Table 2) representative of diverse forest landscapes, disturbance regimes, and composite data characteristics (Figure 3), were chosen in Saskatchewan, Canada.

Across the Taiga Shield ecozone, wildfire is the main driver of forest change (Wulder et al. 2011; Brandt et al. 2013). Forests of relatively low density (Power and Gillis 2006) dominated by white spruce (*Picea glauca* Moench), balsam fir (*Abies balsamea* L.) and black spruce (*Picea mariana* Mill.) are replaced, during early successional stages, by stands of trembling aspen (*Populus tremuloides* Michx.) and balsam poplar (*Populus balsamifera* L.) (Ecological Stratification Working Group 1995). Bogs and fens covered by open stands of tamarack (*Larix laricina* K. Koch) and black spruce are also frequent. Thainka Lake sample area (F), which lies within the Taiga Shield and Reynolds

TABLE 1
Approaches combining spatial context and temporal information for description of change in forest landscape

Approach (description) *Examples*	**Strengths**	**Weak points**
Post-classification comparison Multi-date independent classification *Walter (2004); Kindu et al. (2013)*	• Straightforward comparison • Produces "from-to" results • No need for radiometric normalization	• Only marked discontinuous change identified • Impact/propagation of classifications' errors • Bi-temporal transformations • Potential sliver polygons
Classification of changed areas Difference image is classified *Saksa et al. (2003); Castilla et al. (2009)*	• Simplicity	• Only discontinuous change identified • Threshold of change needed • Bi-temporal transformations
Statistical change of multi-temporal objects Simultaneous segmentation of multi-date image *Desclée et al. (2006); Bontemps et al. (2008); Bontemps et al. (2012)*	• Multi-temporal • Scene independent identification of change/no-change	• Only drastic change identified
Up-/back-dating of reference object map Reclassification of objects identified as changed from a reference *McDermid et al. (2008); Linke et al. (2009); Linke and McDermid (2012)*	• Multi-temporal • Easily updateable • Only changed areas are classified • Categorization of change with logical rules • Linear features captured	• Only discontinuous change identified • Threshold of change needed • Assumes limited number of changes • Human intervention required
Hierarchical spatiotemporal segmentation and temporal trajectory analysis Multi-scale segmentation of temporal trajectory and analysis of spectral trajectory *Gómez et al. (2011)*	• Multi-temporal • Subtle-continuous change is identified • Biophysical interpretation of change • Flexibility conferred by segmentation logic • Copes with incomplete and irregular temporal series • Enables characterization of causal process	• Change is relative
Multi-temporal object linkages Independent segmentation and track of objects' temporal linkages *Hofmann and Blaschke (2012)*	• Multi-temporal • Deal with objects' overlap • Flexibility for analysis	• Difficult interpretation of linkages
Seasonal trend analysis Trend analysis of parameters by object *Parmentier et al. (2014)*	• Identifies spatial pattern of seasonal trends	• Difficult interpretation of parameters • Coarse resolution • Requires interpolation of missing data

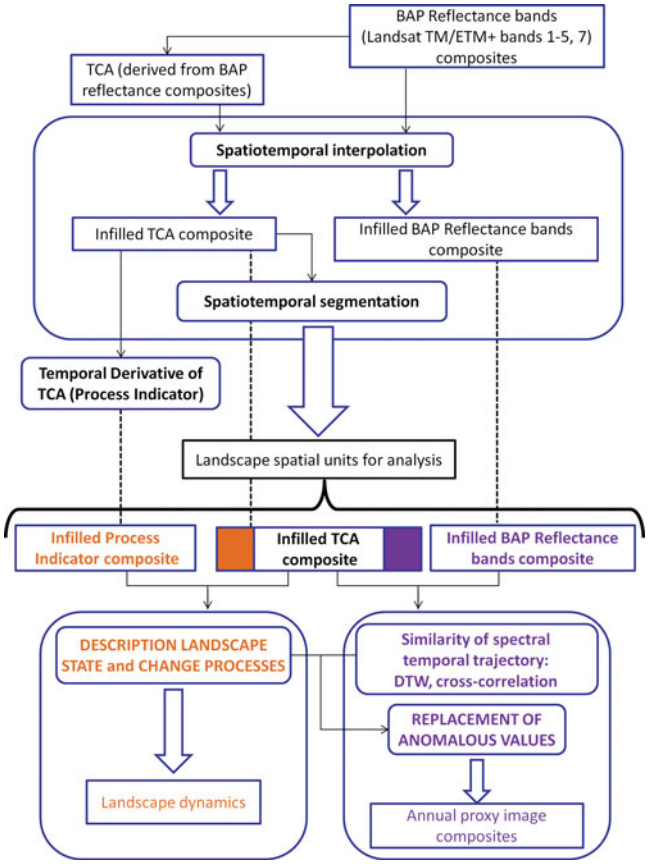

FIG. 1. Schematic representation of the main methods applied for characterization of landscape change and creation of proxy annual image composites.

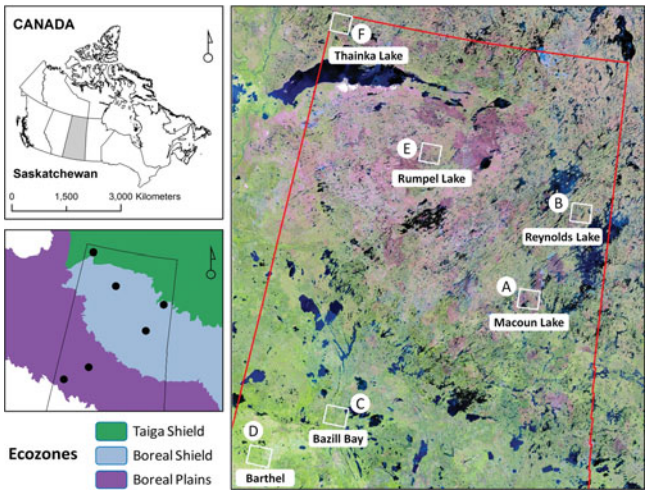

FIG. 2. Location of sample areas in Saskatchewan, Canada.

Lake sample area (B) is in the transition with the Boreal Shield ecozone. In the Boreal Shield, black spruce and jack pine (*Pinus banksiana* Lamb) forests, interspersed with lakes and bedrock outcrops, are also subject to frequent stand replacing wildfires. The southerly sites have more favorable environmental conditions, resulting in higher stand densities and volumes (Power and Gillis 2006) and have more rapid recovery after disturbance than more northerly sites. Rumpel Lake (E) and Macoun Lake (A) sample areas lie within the Boreal Shield ecozone. Two southern samples are located in the Boreal Plains ecozone, a region of Saskatchewan where industrial and agricultural land uses are found, along with active forest harvesting. While pine species dominate these forests, aspen and poplar make the transition to the prairies in the south (Ecological Stratification Working Group 1995). Forestry activities are common in the Bazill Bay sample area (C), whereas the Barthel sample area (D) is located in the interface between forest and agricultural regions.

Figure 3 shows the distribution of Landsat observation frequency in each sample site; note that the majority of pixels have 13–15 observations in Bazill Bay (C) and Barthel (D), with the other sites having less favorable observation frequencies. The BAP composites over all sample areas have a certain amount of pixels with 2 consecutive years of missing data (Table 2), and some sample sites have pixels with 3 consecutive years of missing data. The worst case scenario of 4 consecutive years of missing data, known to be uncommon based on image archive content (White and Wulder 2013) occurs in Macoun Lake (A). In contrast, the Bazill Bay (C) area is representative of near optimal conditions with almost complete coverage during the entire period (1998–2012).

Spatiotemporal Interpolation of Data Gaps

The Tasseled Cap Angle (Powell et al. 2010; Gómez et al. 2011) is a spectral index defined as the arc-tangent of the ratio Greenness (TCG) to Brightness (TCB) of the Tasseled Cap Transformation (Equation 1). TCA images were derived from each annual reflectance BAP composite using the tasseled cap transformation with coefficients for surface reflectance from Crist (1985), resulting in a temporal series of annual TCA image composites. To address gaps due to missing data (resulting either from a lack of available imagery or from clouds and haze), a 3-dimensional spatiotemporal interpolation algorithm was applied (García 2010; Wang et al. 2012) to both the temporal series of annual BAP composites and TCA composites, resulting in complete spatial and temporal coverage of surface reflectance and TCA values (Figure 1). The interpolation algorithm is a penalized least-squares regression based on a 3-dimensional discrete cosine transform (Wang et al. 2012) that maintains the original signal where data exist and minimizes smoothing effects where new data are interpolated.

$$\mathrm{TCA} = \arctan(\mathrm{TCG}/\mathrm{TCB}) \qquad [1]$$

TABLE 2
Characteristics of sample areas and image data composites

Area identifier	Extent (ha)	Composite observations per pixel	Consecutive Years of missing values (% of total pixels)	Ecozone
(A) Macoun Lake	81,634	5–15	4 (2.5%) 3 (18%) 2 (39%)	Boreal Shield
(B) Reynolds Lake	78,551	8–15	4 (0.005%) 3 (2.44%) 2 (12.7%)	Taiga Shield / Boreal Shield
(C) Bazill Bay	86,669	11–15	2 (0.26%)	Boreal Plain
(D) Barthel	88,601	12–15	3 (0.07%) 2 (0.43%)	Boreal Plain
(E) Rumpel Lake	77,332	7–15	3 (10.2%) 2 (43.8%)	Boreal Shield
(F) Thainka Lake	73,721	8–15	4 (0.02%) 3 (0.48%) 2 (22.18%)	Taiga Shield

Although the foundations of the interpolation algorithm are long standing (Whittaker 1923), the use of the algorithm for interpolation is relatively new (Wang et al. 2012), and its performance has not been reported in detail. In order to test the performance of the spatiotemporal interpolation algorithm, we introduced synthetic data gaps into our annual BAP composites and included data gap scenarios that were less favorable than the conditions actually present in our study sites. Spatial and temporal gaps of increasing size (10 % to 40 % of image extent in 1 to 5 consecutive years) were imposed over TCA annual composites, including areas of obvious change and areas of no change. We then evaluated the performance of the algorithm, examining the agreement between the interpolated (predicted) and original (observed; hereafter referred to as reference values)

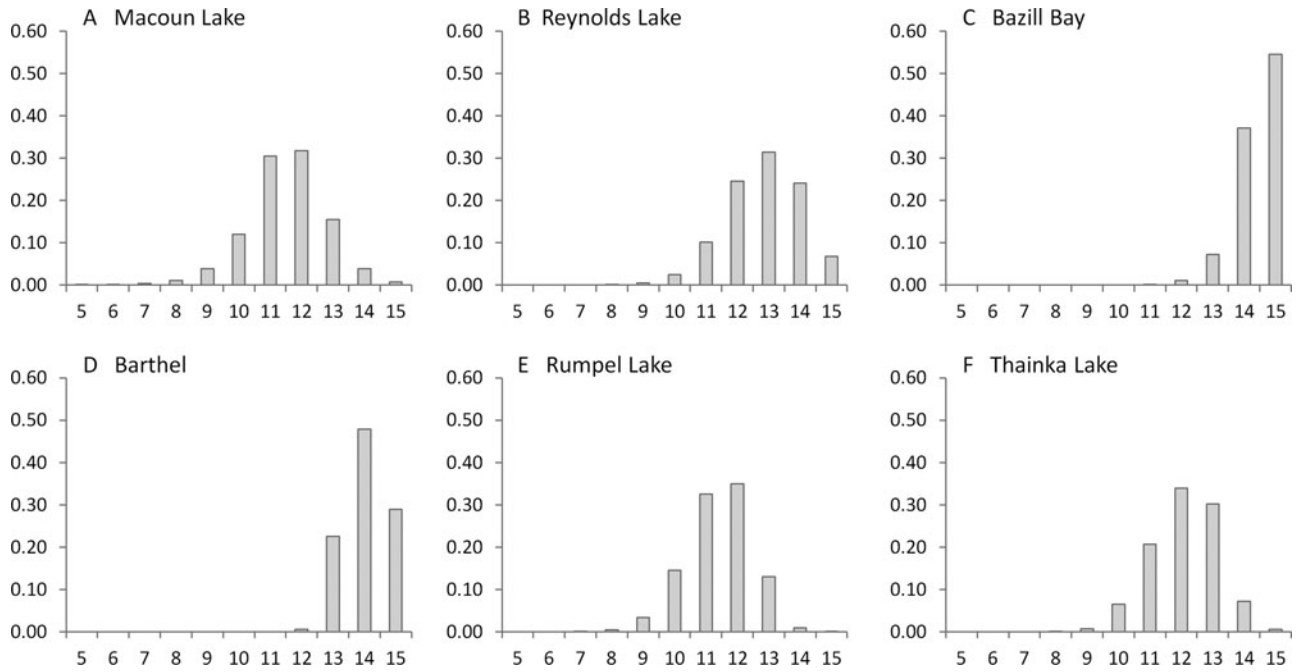

FIG. 3. Frequency of Landsat observations in sample areas. X-axis: number of years with observations; Y-axis: proportion of pixels.

pixel values by examining values of correlation (*R*), RMSE, and bias. As we are interested in assessing the level of association between the reference and proxy values, we use the correlation coefficient (R), not the coefficient of variation (R^2), which is better suited to demonstrating the strength (in terms of variance explained) of predicted values. RMSE provides an indication of the average difference between the reference and proxy values, whilst the bias indicates whether the proxy values are typically lower or higher than the reference values. The effect of the temporal location of the data gap (i.e., missing data in the middle or end of the time series) and the algorithm's performance on reflectance BAP annual composites were also assessed.

Spatiotemporal Segmentation of TCA Image Stack

Spatial units facilitate description, analysis, and reporting of landscape properties such as forest structure, biomass, and change. Phenomenon-driven spatial units were defined by image segmentation of the 15-year TCA image stack (Figure 1). The TCA cube was subject to spatiotemporal segmentation (Gómez et al. 2011) with Definiens Cognition Network Technology®, whereby all layers were given the same weight. Other parameters of the segmentation process (scale = 10, color-shape = 0.9–0.1, and smoothness = 0.5) were selected based on previous experience (Wulder and Seemann 2003; Gómez et al. 2011) and current experimentation. Water bodies (with relatively consistent negative TCA over time) were masked prior to segmentation and excluded from further processing. Resulting objects are by definition contiguous areas that are similar with regard to vegetation and nonvegetation conditions and have followed a similar transformation path over the period of analysis (1998–2012). Given the relatively short period considered and the frequency of data availability, a single-level (opposed to multilevel segmentation described in Gómez et al. 2011) system of landscape units was deemed sufficient for description of forest state and change dynamics. Values of TCA and PI were averaged by object for further analysis.

Characterizing Landscape State and Change Processes

The TCA has been shown to be a reliable indicator of state and change in forest landscapes (White et al. 2011). As a proxy of the proportion of vegetation to nonvegetation, chronosequences of TCA values have been associated with variations in biomass (Powell et al. 2010) and carbon content (Gómez et al. 2012) in coniferous forests. Here, the temporal series of TCA values were used for describing the annual conditions present over forested landscapes. In order to capture detailed change in state condition, a unique scale of TCA values was defined for each site, and 5 or 6 categories were established (depending on local variability) from a comprehensive pool of all dates' values. The TCA categories were defined with a criterion based on the statistical distribution of values, whereby the mean TCA $\pm$ 0.5 and $\pm$ 1.5 standard deviations determine the class boundaries.

At the landscape level, changes in TCA values point to modifications of vegetation density and ecosystem biomass, with temporal series being of value for description of landscape dynamics. Temporal derivatives of the TCA series were evaluated to generate the PI series (Gómez et al. 2011, 2014), where PI values denote the directionality and rate of change in the TCA time series. Aiming to facilitate the identification of change trends and to enable punctual attribution of change rates (i.e., one value at each date), the PI series was generated using smoothed splines of the TCA series. The resultant PI series enable simultaneous identification of positive (e.g., growth) and negative (e.g., stress) processes of forest change. This PI differs from spectral vector change (Malila 1980) in that it provides an instantaneous measure at each time rather than a measure between 2 times. However, to enable identification of discontinuities in the TCA time series corresponding to stand replacing disturbances such as fire or harvest, a 2nd version of PI values was calculated from the original (i.e., unsmoothed) TCA series, making this PI version equivalent to a single-band spectral change vector, that is, a measure of directionality and rate of change between 2 times (in our case 2 consecutive years). With this combined approach of temporal derivatives, the PI calculated over the smoothed curve characterizes trends and provides a value of change process at each measured date, whereas the PI calculated from the original TCA series identifies discrete transformations that occur within a single year (i.e., disturbances are located with a temporal precision of 1 year).

A unique scale of PI values for simultaneous description of discontinuous change and subtle transformations applicable to any forest system regardless of canopy cover would be of paramount interest. However, the rate of variation in spectral response associated with successional processes varies according to vegetation structure, species composition, and site quality. Therefore, PI values are not universal and cannot be directly compared among different sites. However, stand replacing disturbances characterized by a strong decline in reflectance (Schroeder et al. 2011; Goodwin and Collett 2014) can be identified by a sudden and marked decrease of TCA in the temporal trajectory (i.e., a discontinuity of the series), concomitant with the highest negative PI values. In temporally normalized TCA series (i.e., each year's TCA pixel value divided by its temporal average), values of PI at discontinuities represent a similar process of change. In our study area, we found that a PI threshold of –0.30 in normalized TCA series was proficient to identify stand-replacing disturbances and to map Time Since Disturbance (TSD; results not shown). This threshold was established by pooling a comprehensive sample of objects from a range of land cover types as identified in a circa 2000 land cover product for Canada developed under the project Earth Observation for Sustainable Development (EOSD; Wulder, White, Cranny, et al. 2008).

For characterization of continuous processes of change, PI scales were defined at each site by pooling all PI values. To facilitate ecological interpretation, 5 categories of change poten-

tially associated with successional processes (i.e., fast change by stress, slow change by stress, stability, growth, and fast growth) were related to PI intervals. For definition of PI intervals, a criterion based on data distribution was applied whereby class boundaries are defined by the mean PI $\pm$ a number of standard deviations. The appropriateness of PI scales and associated thresholds were supported by visual inspection of the original image composites.

Temporal TCA and PI trajectories of individual objects were analyzed for description of the landscape change dynamics over the 15-year period (1998–2012). A spatial database of annual state and change processes was compiled and interrogated for spatial location and temporal identification of the dynamics of interest. Annual maps of state and ongoing change processes were visualized and statistics summarized, enabling the analysis and comparison of patterns and distribution of forest condition, change events, and subtle transformations.

Detection and Replacement of Anomalous Pixel Values

After implementing the gap-filling process described previously, BAP composites are free of data gaps and enable characterization of landscape dynamics (as described in the previous section). However, for modeling applications based on individual pixel trajectories, the quality and consistency of image composites benefit from refining approaches (e.g., Hermosilla et al. 2015). In order to check the composites' consistency, individual pixel trajectories were examined with an automated approach. Pixels with TCA trajectories that were not consistent with local landscape processes (as defined by the spatiotemporal segment within which the pixel is located) may represent anomalous values resulting from the compositing process (e.g., delayed change detection—whereby the change happens outside the compositing day-of-year (DOY) window for a given year—or atmospheric contamination by undetected cloud, haze, or smoke). They may also correspond to a unique landscape feature (e.g., bedrock outcrop in a closed canopy forest).

We explored the capacity of time-series similarity analysis to automatically identify pixels with spectral anomalies resulting from delayed change detection and residual atmospheric contamination. Each pixel TCA trajectory was compared with the average trajectory of its parent object using 2 time-series similarity measures: the dynamic time warping (DTW) algorithm and the cross-correlation. DTW was evaluated with various parameter configurations (i.e., symmetric and asymmetric window step pattern, and unconstrained end; Giorgino 2009) providing values of *global distance* (i.e., an overall value of similarity) and *best partial alignment* (bpa) indicative of the trajectories' best aligned length. The maximum value of cross-correlation and its *argument*, which indicate the point in time when the trajectories are best aligned and enable identification of a possible time delay between two trajectories, were also considered. For reference, greatest similarity of spectral series was defined as a combination of a low DTW global distance value, a long duration of best partial alignment, and a maximum cross-correlation value at time lag zero (i.e., argument 15) (e.g., Figure 4a). Deviations from our defined similarity reference indicate local spectrotemporal irregularities, some of which may be associated with anomalies resulting from the image compositing process.

Pixels with low values of DTW global distance, high bpa, and a 1-year lag in their maximum cross-correlation values (i.e., argument 16) were interpreted as indicators of delayed change detection in the composite (Figure 4c, d). Low DTW global distance values and the duration of bpa (Tormene et al. 2009) helped identify anomalous pixel values by atmospheric residual effects (Figure 4e); in this case, a remarkably increased DTW *normalized cumulative distance* (Giorgino 2009) at a given date provides conclusive information and points to the date of anomaly. Ideally, other pixel qualities can be informed by the similarity analysis; for example, pixels with a temporal trajectory significantly different to the surroundings, as indicated by short bpa and high DTW global distance may correspond to a unique landscape feature (e.g., bedrock outcrop in forest; Figure 4f). Various flags were generated to relate the nature of the original composite pixels for later consideration (Table 3). Similar to missing values or data gaps, anomalous observations were replaced using spatiotemporal interpolation of eligible observations in both the TCA and reflectance temporal composites, resulting in more consistent wall-to-wall products for use in other applications.

RESULTS

Spatiotemporal Interpolation of Data Gaps

We evaluated the performance of the spatiotemporal interpolation algorithm in order to determine its ability to fill synthetic data gaps of increasing size and persistence (increasing consecutive years of missing data) in TCA annual series (Figure 5a). Additionally, we evaluated the algorithm's performance when interpolating annual time series of reflectance composites (Figure 5b). Our analyses indicated that the performance of the interpolation algorithm was highly dependent on the nature of the data gaps (Figure 5a, Table 4). For example, considering a data gap equivalent to 10 % of the image area, as the gap increased in duration (1 to 5 consecutive years), values of R decreased ($R = 0.975$ for a 1-year temporal gap versus $R = 0.825$ for a 5-consecutive-year temporal gap) and RMSE increased (RMSE $= 0.022$ to RMSE $= 0.060$; Table 4). Spatial gaps of increasing size (10 % to 40 % the image area) had a similar effect, with a lower magnitude relative to the impact of temporal gaps. For example, consider a 10 % spatial gap in 1 year ($R = 0.975$, RMSE $= 0.022$) compared to a 40 % spatial gap over 1 year ($R = 0.945$, RMSE $= 0.046$). Bias typically increases with increasing size of spatial gaps and was relatively small and consistently negative for 3- and 4-year gaps (regardless of gap size). Despite decreasing R and increasing RMSE when the spatiotemporal gap increases, agreement between predicted and reference data remains over 85 % when 20 % spatial gaps persist for more

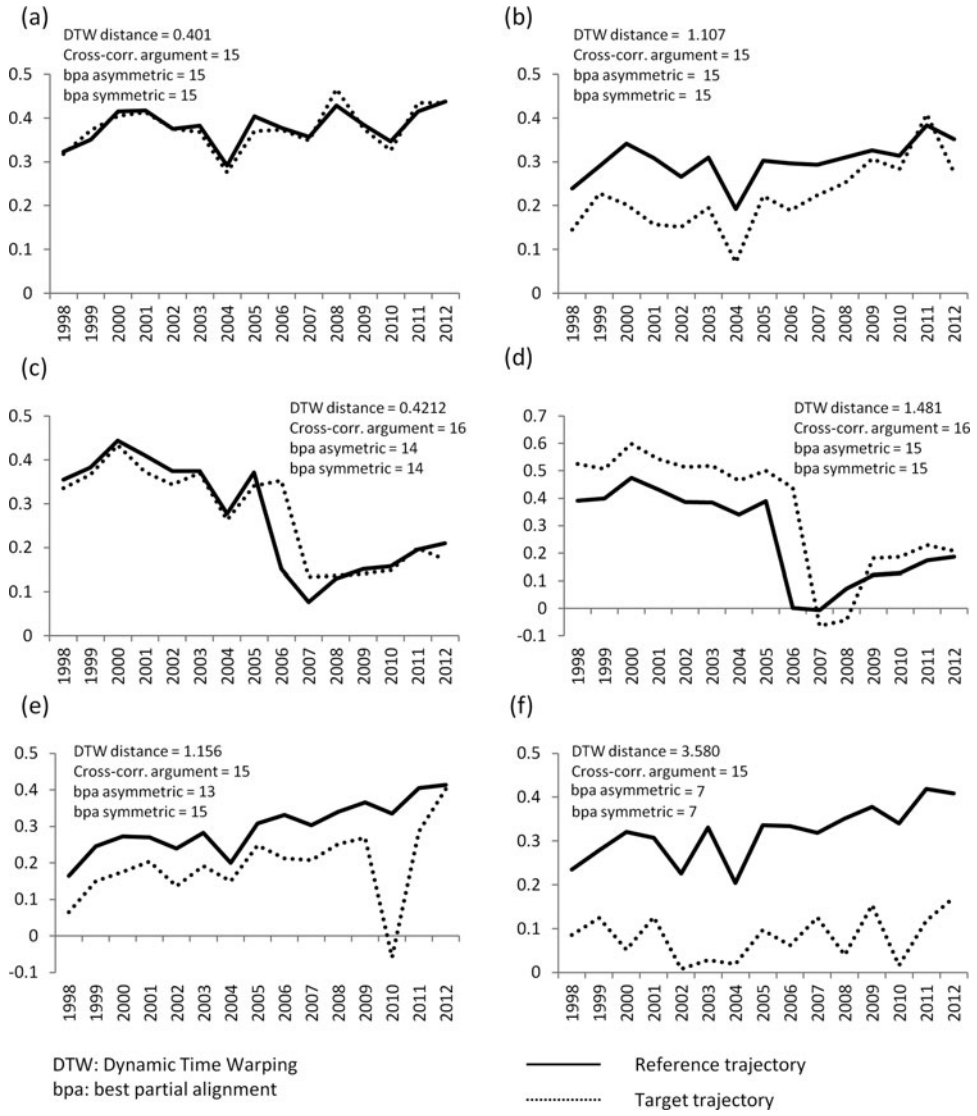

FIG. 4. Samples of TCA time-series similarity analysis. (a, b): Expected similarity with maximum cross-correlation nonlagged (argument 15). (c, d): Anomalous pixel due to delayed disturbance detection, identified by cross-correlation lagged +1 (argument 16) and long best partial alignment in the symmetric and asymmetric window patterns. (e) Anomalous pixel by residual atmospheric feature identified by differing best partial alignment in the symmetric and asymmetric window patterns. (f) Land-cover dissimilarity (unique landscape feature) identified by large DTW global distance and short best partial alignment.

than 3 consecutive years. Although the temporal location of a 1-year data gap did not impact the interpolation performance (Figure 5c); when two or more consecutive years were missing, R and RMSE values were less favorable than similar scenarios in the middle of the series. For instance, comparing the filling of a 4-consecutive-year data gap in the middle of the time series (years 5 to 8), with an initial (years 2 to 5) and final (years 11 to 14) gap, the agreement between predicted and reference values varies ($R = 0.86/0.84/0.81$ and RMSE $= 0.05/0.06/0.05$). The interpolation of data gaps in reflectance band composites had lower R values for the visible bands 1, 2, and 3 ($R < 0.90$) and higher R for bands 4, 5, and 7 ($R > 0.95$) (Figure 5b, Table 5). RMSE was largest for band 4 and smallest for band 1. Bias was small and negative for all spectral bands except band 1, indicating that proxy values were typically higher than the reference values, except for band 1 (Tables 4, 5).

The 3D character of the interpolation (Figure 6) enabled infilling of values at end dates of the time series (i.e., temporal boundary) and image borders (i.e., spatial boundary). Temporal spectral profiles of infilled pixels proved the effective consideration of both temporal and spatial dimensions for proficient nonlinear interpolation.

TABLE 3
Values of the flag raster layers characterizing the quality of original composite pixels, including identified spectrotemporal anomalies

Value	Definition
0	Good value
1	Single date missing value
2	Two or more consecutive missing values in middle of series
3	Anomaly by delayed change detection

Spatiotemporal Segmentation of TCA Image Stack

The process of image segmentation generated spatial units as characterized in Table 6. Objects derived by spatiotemporal segmentation of the TCA image (69.5 ha on average) are practical units for analysis and reporting of change locally, providing detailed spatial information of forest state and ongoing processes.

Characterizing Landscape State and Change Processes

Global average TCA values at each site describe the overall proportion of vegetation to nonvegetation during the entire period (1998–2012; Figure 7a). Samples in the Boreal Plains (Bazill Bay and Barthel) show significantly higher values of TCA, reflecting more favorable conditions for developing denser vegetation coverage. There is no major difference in global TCA values between the Taiga Shield (Thainka Lake and Reynolds Lake) and the Boreal Shield sites (Rumpel Lake and Macoun Lake) (Figure 7a), indicating similar proportions of vegetation to nonvegetation during the period considered and despite typical differences in the site quality between ecozones. Rumpel Lake site recorded the lowest global TCA value (Table 7); from the initial date, the overall TCA here trends slightly upward, indicating vegetation recovery from large wildfires that occurred in and prior to 1998 (Canadian Forest Service 2013) (Figure 7b). Significant changes in the overall proportion of vegetation to nonvegetation occurred in Reynolds Lake in 2000–2001 and in Macoun Lake in 2005–2006, as consequence of large fire events and remarkable decline of TCA is obvious in Bazill Bay and Barthel after 2000, with minimum values in 2003.

Overall, values of the PI for the period 1998 to 2012 (Figure 7c) point to vegetation decline or stress (high negative PI) in Thainka Lake and Macoun Lake, stability or equilibrated change (overall PI close to zero) in Reynolds Lake, and growth (high positive PI) in Rumpel Lake, Barthel, and Bazill Bay. Examining the chronosequence of average PI values (Figure 7d), we found high negative values in 2001 and 2002 for Reynolds Lake, and in 2003 and 2004 for Thainka Lake, associated with large wildfires in these areas. Equally high negative PI values occurred in 2001 and 2002 in Bazill Bay and Barthel areas and were associated with high mortality rates of aspen in this region, as consequence of an extreme drought (Bonsal and Regier 2007). After 2003, the increase of vegetation density (PI > 0) in the Barthel and Bazill Bay sites surpassed previous decline. Relatively high values of PI standard deviation indicate significant variability of change processes in the Barthel area (Table 7),

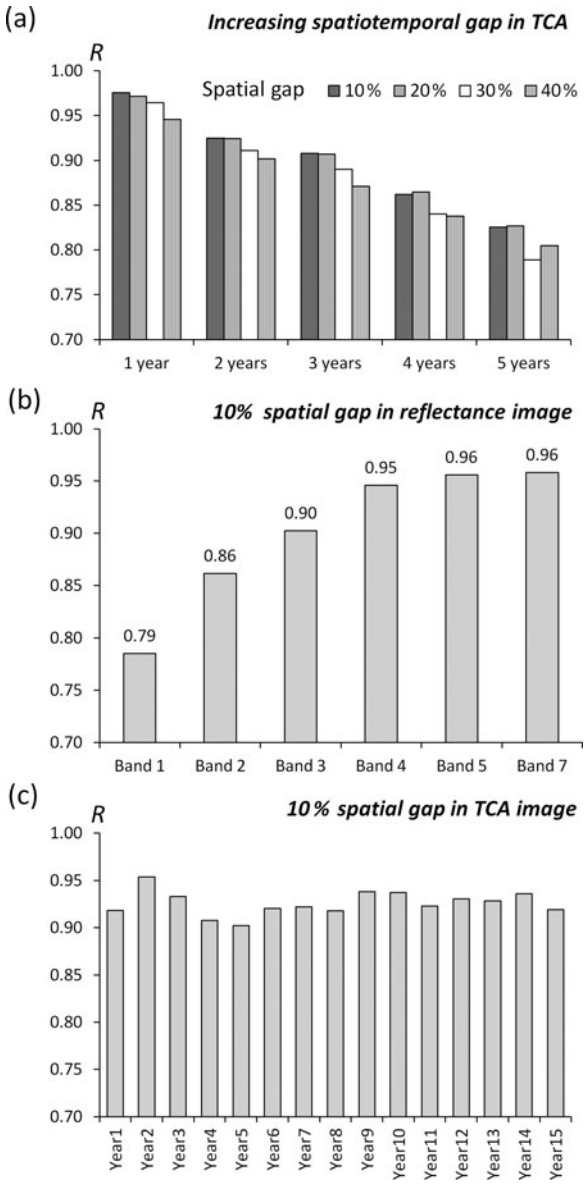

FIG. 5. Evaluation of the spatiotemporal interpolation performance with Pearson's *R*. (a) Agreement with reference of TCA values after interpolation of synthetic data gap covering 10 % extent of image in 1 to 5 consecutive years; (b) Agreement with reference of individual Landsat reflectance bands after interpolation of synthetic 10 % extent of image spatial gap; (c) Agreement with reference of TCA after interpolation of synthetic gap covering 10 % extent of image in a single year.

TABLE 4
Results of spatiotemporal interpolation performance assessment in different scenarios of consecutive years' data gaps and spatial gaps (TCA)

	10% spatial gap			20% spatial gap			30% spatial gap			40% spatial gap		
	R	RMSE	Bias	R	RMSE	Bias	R	RMSE	Bias	R	RMSE	Bias
1 year (year 7)	0.975	0.022	0.0004	0.971	0.027	−0.0004	0.964	0.031	−0.0022	0.945	0.046	−0.0006
2 years (years 6–7)	0.924	0.039	0.0033	0.924	0.047	0.0044	0.911	0.052	0.0043	0.901	0.062	0.0080
3 years (years 5–7)	0.907	0.048	−0.0188	0.907	0.059	−0.0235	0.890	0.066	−0.0276	0.871	0.072	−0.0211
4 years (years 5–8)	0.862	0.054	−0.0031	0.864	0.065	−0.0098	0.840	0.072	−0.0144	0.837	0.079	−0.0110
5 years (years 5–9)	0.825	0.060	0.0037	0.826	0.069	0.0018	0.789	0.078	0.0020	0.804	0.085	0.0036

where stand replacing disturbance (harvesting) is followed by regeneration. Furthermore, a 4-year cycle is evident in the overall landscape processes (Figure 7d). Cyclical trends of prevalent change processes are less pronounced in the 2nd half of the study period, possibly in relation to a reduction in provincial harvest since 2004 (Saskatchewan Ministry of Environment 2012).

Histograms of the overall distribution of processes (Figure 8a) are constructed relative to local ecosystem conditions, i.e., defined with site-dependent PI intervals. The shape of the histograms, and the values of skewness and kurtosis (Table 7), point to different landscape change dynamics in sample areas. For instance, a normal distribution with a mean of zero and little spread (e.g., Rumpel Lake) indicates overall stability (negative changes such as disturbance are offset by positive changes such as growth). A hump within the PI intervals indicative of growth or stress suggests some prevalence of these processes during the period (e.g., Reynolds Lake, Bazill Bay). An extended distribution relates a dynamic landscape with processes of change balanced (e.g., Bazill Bay). In contrast, the distribution of processes in Rumpel Lake, characterized by high kurtosis value, suggests the existence of a few extreme events responsible for the variability in this landscape area.

TABLE 5
Results of spatiotemporal interpolation performance assessment in different reflectance bands for a 10% extent gap

Band	R	RMSE	Bias
1	0.785	0.0053	0.00004
2	0.861	0.0060	−0.00081
3	0.902	0.0054	−0.00002
4	0.946	0.0215	−0.01067
5	0.955	0.0168	−0.00817
7	0.958	0.0109	−0.00271

As demonstrated, landscape values of global PI may be similar, yet can relate different landscape dynamics (e.g., negative PI responding to fire or gradual decline caused by drought or disease). Locally, specific processes of change may be distinguished by PI temporal trajectories as they diverge according to the nature of change: forest stands affected by drought or disease will typically have several consecutive years of low negative PI values (i.e., slow change), whereas stand-replacing disturbances typically manifest as sudden and highly negative PI, associated with the magnitude and relative speed of these fast-changing events.

Temporal summaries facilitate examination of landscape-change dynamics, identifying prevalence of processes and temporal distribution of change, and unveiling a diversity of patterns that could be associated with local conditions (e.g., land use, weather). Summaries in Bazill Bay and Barthel, the southernmost sample locations, exhibited similar change dynamics over time (Figure 8b). Both sites were mostly stable but appeared affected by drought in 2001 and 2002, to which vegetation in Bazill Bay was slower to recover relative to vegetation in Barthel (Figure 8b). In Rumpel Lake, extensive areas increased the proportion of vegetation to nonvegetation at various dates—as per high positive PI values in 1999, 2005, and 2011—while global TCA values remained low (Figure 7d): this is likely explained by the vigorous recovery of shrubs and open stands of coniferous after disturbance. Figure 9 portrays the spatial distribution of processes over time in Bazill Bay (C), where the landscape is dominated by subtle processes of growth and stress, and Reynolds Lake (B), where discrete and drastic events occurred during the study period.

Detection and Replacement of Anomalous Pixel Values

The majority of pixels (68.46 %) examined had spectral trajectories that were notably similar to the average trajectory of

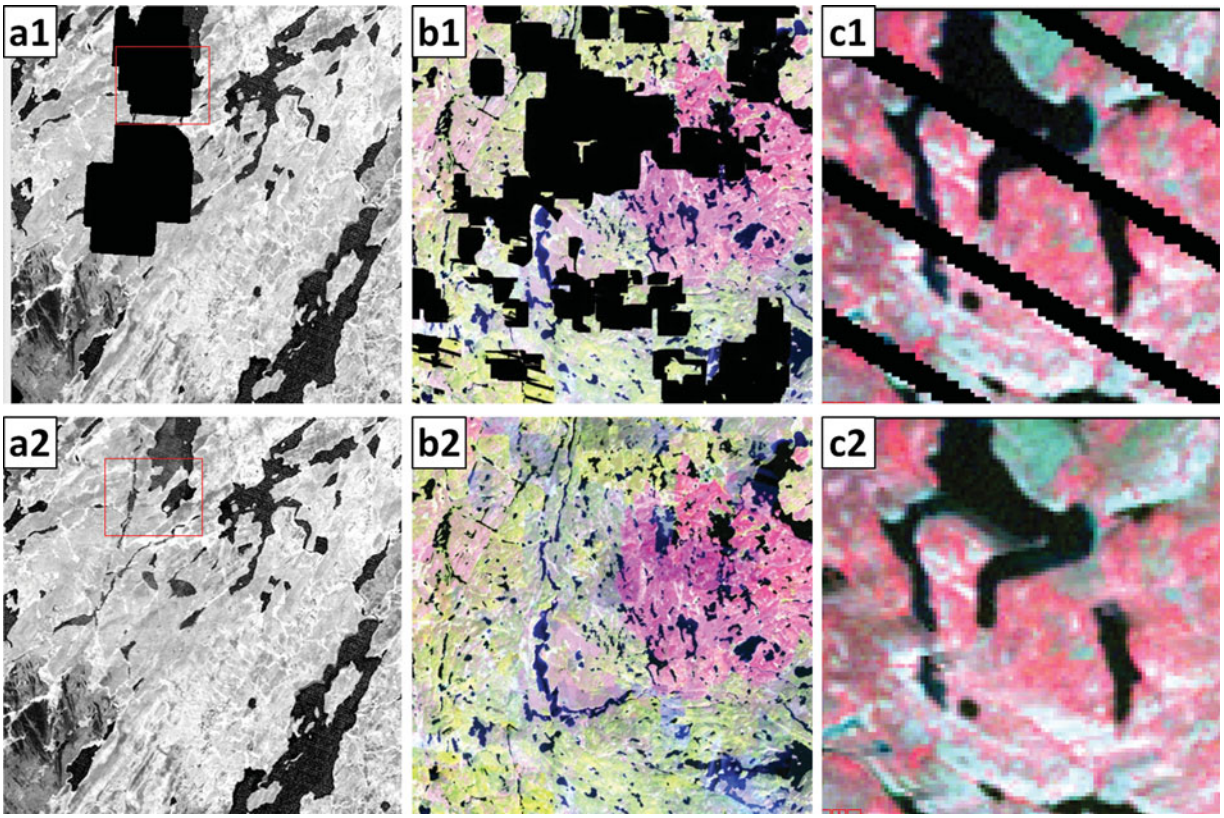

FIG. 6. Examples of the spatiotemporal interpolation. (a1, a2): TCA composite before and after, respectively, interpolation. (b1, b2): Reflectance composite before and after, respectively, interpolation of an extensive data gap by lack of observations. (c1, c2): Reflectance composite before and after, respectively, interpolation of stripped data gap typical of Landsat 7 ETM+ SLC-off.

the pixel's neighbourhood (Table 8). We identified composite anomalies corresponding to delayed detection of a disturbance event in 0.37 % of the inspected pixel trajectories, when the maximum cross-correlation was lagged by +1 (i.e., argument 16) and the DTW bpa was ≥14 for both the symmetric and asymmetric window patterns (e.g., Figure 4c, d). Residual atmospheric contamination was indicated for 2.31 % pixels with low DTW global distance, maximum cross-correlation at lag zero, and bpa asymmetric << bpa symmetric. The date of anomalies was marked by a remarkably increased DTW normalized cumulative distance (Giorgino 2009).

TABLE 6
Characteristics of spatial units resulting from image segmentation

	Spatial segments (objects)	
Sample site	Number	Mean ± stdev area (ha)
(A) Macoun Lake	843	74.7 ± 65.5
(B) Reynolds Lake	775	86.9 ± 66.9
(C) Bazill Bay	1042	79.1 ± 79.1
(D) Barthel	1481	58.7 ± 67.5
(E) Rumpel Lake	794	84.1 ± 59.9
(F) Thainka Lake	1839	33.4 ± 25.4

The parametric configuration of DTW and cross-correlation similarity measures aimed to identify anomalous values related to the BAP composite generation, in particular those anomalies leading to delayed change detection and residual clouds. As a byproduct of this process, the analysis pointed to other qualities of pixel values, although exhaustive exploration was beyond the scope of this study. The parametric configuration of the similarity analysis left around 25 % of pixels' trajectories unexplained (Table 8); with a less strict criterion for trajectory similarity (i.e., bpa ≥ 10), 80 % of pixels would fall into the "expected" category, suggesting more research is needed into parametric tuning and the utility of time-series similarity measures for assessment of time-series quality. We evaluated these results qualitatively, with visual inspection of all pixels identified as anomalous through the 15-year time series. The majority of those identified as anomalous by delayed change detection were confirmed correct, but a few appeared scattered on the boundary of a water body. Those categorized under residual

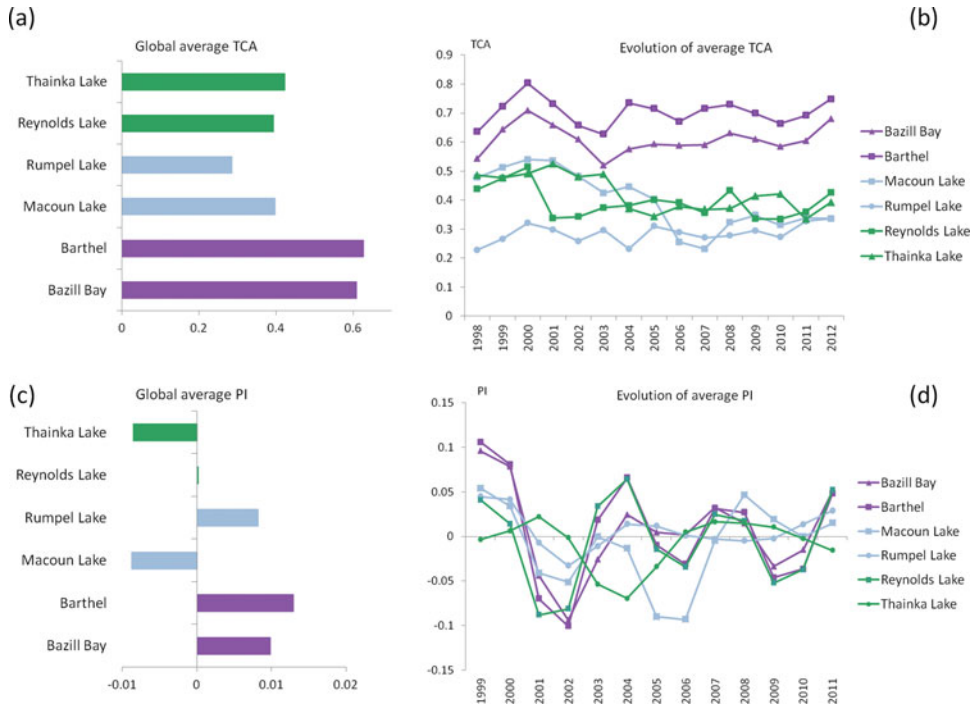

FIG. 7. Values of TCA and PI in sample areas. (a, c): Overall values for period 1998–2012. (b, d): Evolution of average values during period 1998–2012.

atmospheric anomaly included clouds, but also shadows, and eventual water bodies.

DISCUSSION

In this study, we used a 15-year (1998–2012) time series of annual Landsat BAP composites (White et al. 2014) as a source of information for landscape-level characterization of change in Saskatchewan, Canada. The frequency of BAP observations in the time series, all of which were captured during the growing season (1 August ± 30 days), varied by sample site, with a greater number of data gaps found in areas of persistent cloud cover. Data gaps were filled using a spatiotemporal interpolation algorithm that preserved existing observations, enabled wall-to-wall data coverage, and minimized uncertainties that typically remain with interpolations operating in either the temporal or spatial domains exclusively (Huang et al. 2010; Zhu et al. 2012). We documented how the performance of the spatiotemporal interpolation algorithm varied according to the characteristics of the data gaps (e.g., spatial extent, temporal extent, and temporal location in the time series). Spatial data gaps of 4 or more years representing 20 % of the pixels within the study unit were reliably filled by the algorithm, providing that supportive spectral data existed in years before and after the temporal gap. As expected, the reliability of the composite in interpolated areas decreases with increasing size (both spatial

TABLE 7
Statistical values of TCA and PI indices for land areas in each sample site

	Macoun Lake (A)	Reynolds Lake (B)	Bazill Bay (C)	Barthel (D)	Rumpel Lake (E)	Thainka Lake (F)
TCA mean	0.398	0.393	0.609	0.627	0.285	0.423
TCA stdev	0.150	0.112	0.115	0.161	0.106	0.129
TCA skewness	−0.636	0.158	−0.801	−1.178	−0.589	−0.999
TCA kurtosis	0.343	1.260	2.011	1.213	0.167	1.071
PI mean	−0.008	0.002	0.014	0.014	0.009	−0.006
PI stdev	0.066	0.062	0.058	0.088	0.035	0.056
PI skewness	−0.975	−1.248	−0.610	0.522	−1.574	−1.282
PI kurtosis	1.519	3.042	3.121	4.624	7.382	3.307

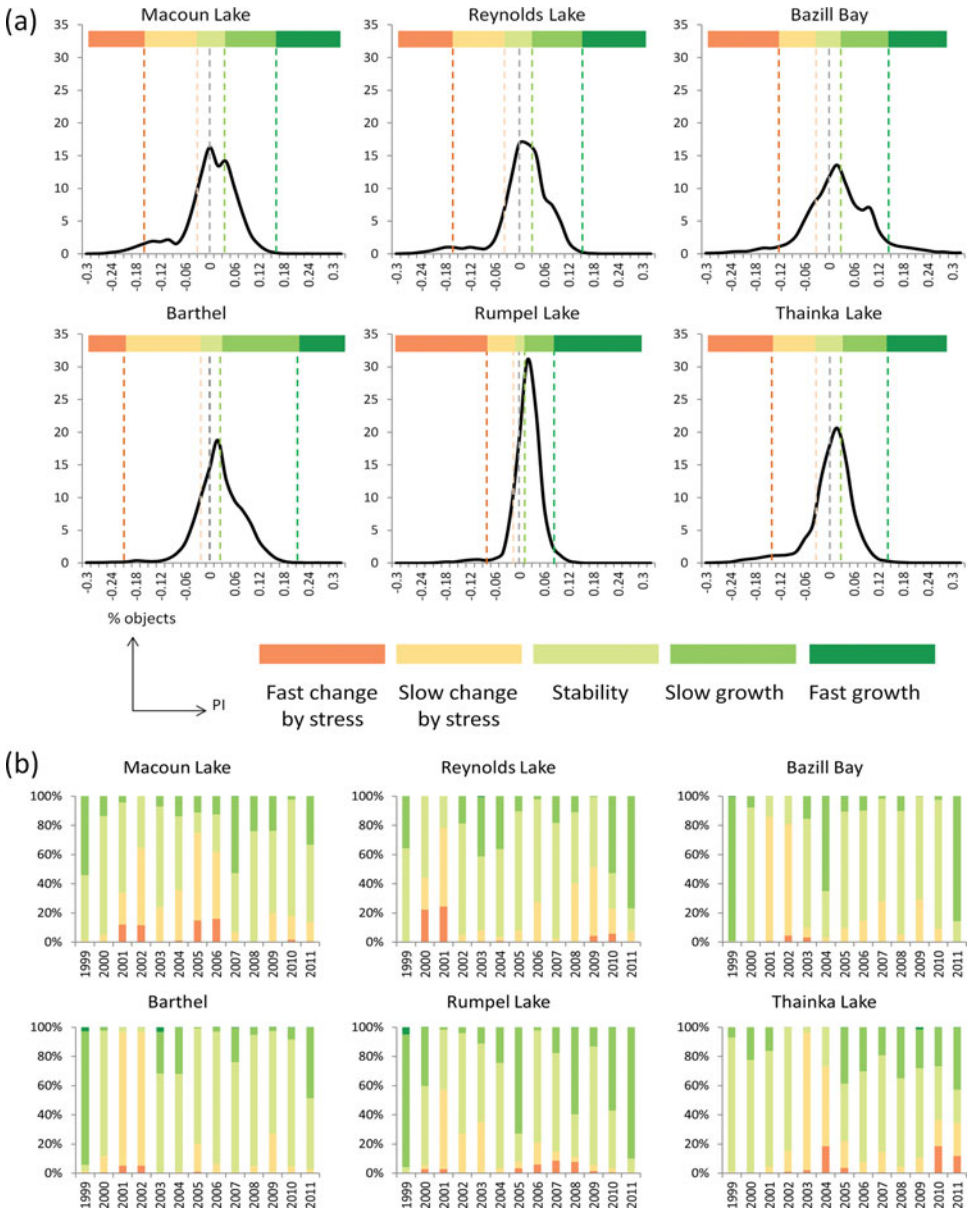

FIG. 8. (a) Overall distribution of processes in sample sites, indicating a range of landscape dynamics during the study period (1998–2012). (b) Proportion of area undergoing processes by year.

and temporal) of the data gap. Three-dimensional interpolation methods, such as that demonstrated herein, provide a means for filling gaps in pixel-series for locations where data availability is limited (for the variety of reasons we have identified herein).

When compared to the use of single scenes, BAP image composites are advantageous because they afford seamless coverage over very large areas. A temporal stack of wall-to-wall, annual data enable identification of otherwise nondetected changes. When generating BAP image composites for large areas, standardized protocols for radiometric and atmospheric correction, (e.g., LEDAPS; Masek et al. 2006), and cloud detection (e.g., Fmask; Zhu and Woodcock 2012; Zhu et al. 2015) are necessary. The reliability of image composites for land cover and change, biomass estimation, and carbon modeling over large areas is of paramount interest (e.g., Potapov et al. 2011; Griffiths, Van der Linden, et al. 2013; Griffiths, Kuemmerle, et al. 2013). Annual composite products, which have a greater likelihood of residual clouds when compared to multiyear composites (Broich et al. 2011), facilitate time series analysis and thereby can provide increasingly improved results for change detection and forest structural characterization. The restriction of pixel observations

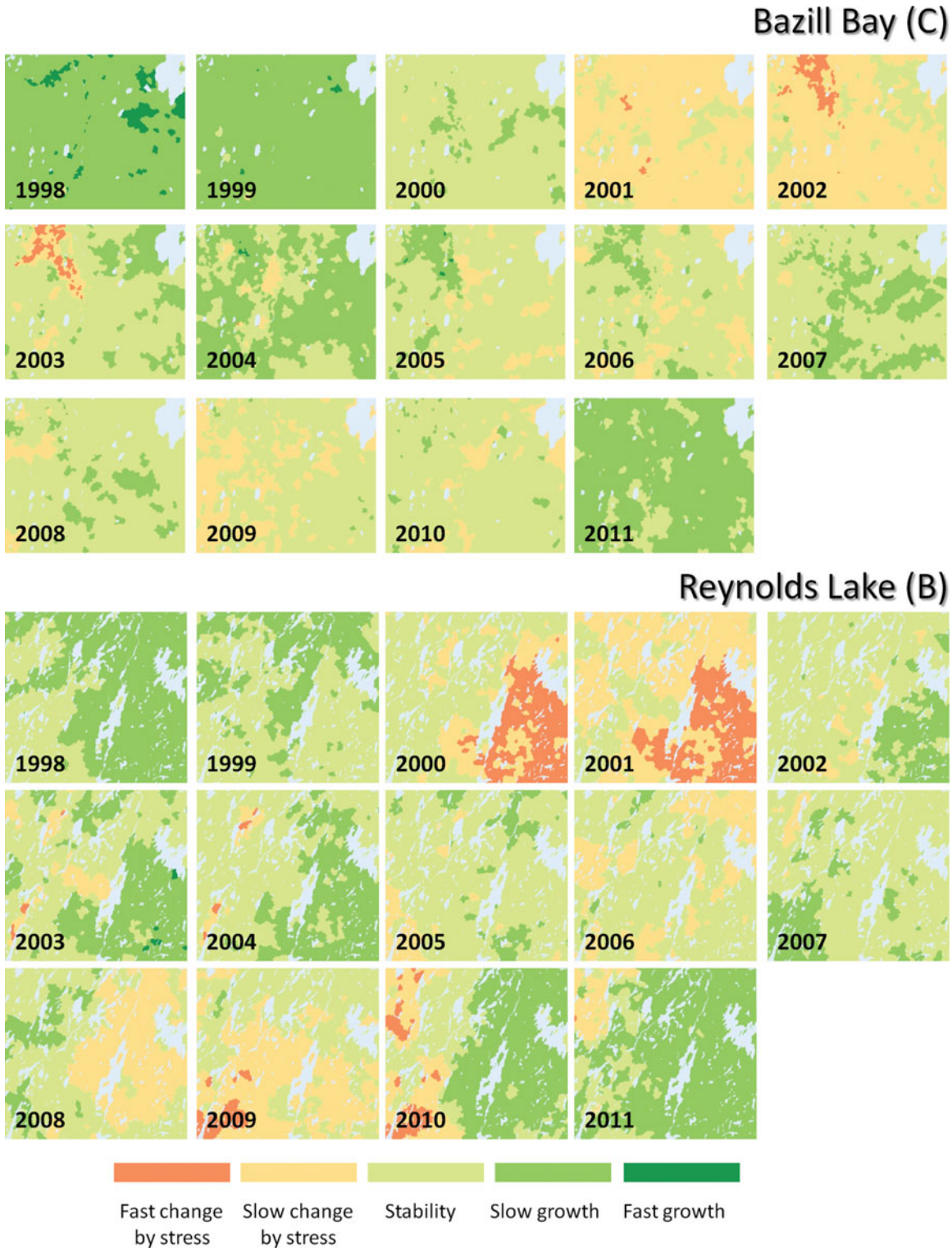

FIG. 9. Processes of change over time occurred during the study period in Bazill Bay (C) and Reynolds Lake (B).

TABLE 8
Quality of pixels characterized by the time-series similarity analysis using dynamic time warping and cross-correlation measures

Pixel Quality	Similarity Measures	Proportion (%)
Expected: trajectory similar to average neighborhood	Low DTW global distance Max. cross-correlation non-lagged bpa asymmetric $\geq$ 12 bpa symmetric $\geq$ 12	68.46
Anomaly: delayed disturbance detection	Low DTW global distance Max. cross-correlation lagged + 1 bpa asymmetric $\geq$ 14 bpa symmetric $\geq$ 14	0.37
Anomaly: residual atmospheric feature	Low DTW global distance Max. cross-correlation non-lagged bpa asymmetric << bpa symmetric Cumulative distance	2.31
Land cover dissimilarity: unique landscape feature	Large DTW global distance Short bpa	3.78

Note: bpa = best partial alignment calculated with the DTW.

to those acquired during the growing season aims to minimize reflectance discrepancies due to phenology and sun angle differences. Furthermore, with an object-based approach for analysis of change, the impact of residual cloud patches (i.e., those not detected by Fmask) should be reduced by averaging of pixel values within objects. Nevertheless, phenological disparities or atmospheric anomalies such as cloud and haze can persist in image composites (as well as mosaics and single scenes), complicating landscape change detection. The spatiotemporal segmentation approach was used not only to provide spatial context for change detection, but also to aid in the identification of anomalous pixel values, such as delayed change detection or residual cloud (or haze) not detected with Fmask. Our analysis of the similarity of spectral trajectories, implemented through DTW and cross-correlation measures, provided valuable information about the quality of the composite as well as detecting anomalies for replacement. The approach was implemented using real data, reducing some of the options synthetic data provide (e.g., exhaustive accuracy assessment) and yielded correct but not fully conclusive results. Some issues requiring further investigation were apparent during the current implementation: the best trajectory length for detecting anomalies while balancing computing effort, a need to evaluate omission error (i.e., amount of undetected anomalies), and the adequacy of the reference units for comparison (i.e., objects). Additional research could be implemented to increase our understanding of the pixel quality as indicated by parametric combinations of similarity measures and to further benefit from the contextual time series analysis. As demonstrated, combining spatial and temporal traits of spectral trajectories enables gap-filling of annual BAP composites for use in a range of forest monitoring applications.

Time-series approaches have shown to be effective for characterization of change in forest landscapes (Kennedy et al. 2012; Potapov et al. 2012; Goodwin and Collett 2014), with some advantages over bi-temporal methods that rely on paired images–or multi-year composites in the case of large areas. For example, time series analyses can inform on trends and rates of change (Goodwin et al. 2008) rather than solely characterizing the presence or absence of change. Time-series approaches are capable of supporting the characterization of a broader range of processes (Gillanders et al. 2008) and change patterns (Gómez et al. 2014). With appropriate data available via direct observation or modeling, trend analysis becomes valuable for describing subtle and continuous processes (Eastman et al. 2009; Parmentier et al. 2014). In our analysis, we combined an annual series of spectral data with an object-based approach for characterizing change dynamics at the landscape level, relying on the TCA and its temporal derivative, the PI. TCA is a proficient spectral index for detecting land cover change (White et al. 2011), modeling biomass over time (Powell et al. 2010) and characterizing carbon pooling dynamics (Gómez et al. 2012). As an indicator of the proportion of vegetation to nonvegetation, variations in TCA can characterize changing density in forests, and while global values can identify development or deterioration of overall ecosystem condition, local trends and patterns of PI over time identify processes and facilitate inference of the type, magnitude, and agent of change. For example, some sample sites in Saskatchewan showing overall high negative PI values at one date were affected by fires with complete cover removal, whereas other samples had similar overall high negative PI values resulting from drought stress. Simultaneous interpretation of forest condition with the TCA and change process with the PI enables distinction of the type and disturbance agent, because they produce different spectral responses in forest stands (Hais et al. 2009; Schroeder et al. 2011). For assessment of carbon budgets, it becomes relevant to identify perturbation intensity and forest condition prior to disturbance, because both factors influence the NEP recovery rate (Taylor et al. 2014). The accuracy of subtle and progressive change is difficult to assess (Olofsson et al. 2014), particularly in historical series where no auxiliary data exist. In the absence of more detailed or accurate information, self-consistency and data evidence are the most reliable available tools. Furthermore, the potential impact of phenological effects during the summery 60-day envelope of our BAP composites is presumably different depending on land cover type (e.g., coniferous or deciduous forests, grasslands) and de-

pending on the spatial scale of analysis. For example, a few pixels' observations at the start or end of the allowable compositing period may affect a small object but may be irrelevant as part of a larger one. Indeed, per-pixel and local analysis would benefit from inspection of phenological effects on TCA and annual PI trajectories, and time-series similarity measures might play an important role in determining the magnitude of phenological impacts.

Combining the strengths of continuous and discrete approaches, temporal derivatives of the smoothed and original spectral signals enabled identification of subtle change and precise dating of disturbance. As a derivative of a smoothed and adjusted curve (e.g., spline), PI values indicate the instantaneous rate and directionality of change at measured dates, and by means of this continuous technique, trends of change are also identified. For time-series analysis, splines are superior to other continuous methods (e.g., wavelets) in providing the analytical adjusted function and its derivative value at any time, so that ongoing processes can be determined. However, continuous methods are not optimal for detecting temporal discontinuities in spectral response corresponding with stand-replacing disturbance. For identification of stand-replacing disturbance with annual time precision, a temporal derivative of the original TCA trajectory is most effective, evaluating change by annual intervals. Through a scale of temporally normalized TCA trajectories, a unique value of PI identifies drastic transformations in various ecozones and for a range of disturbance regimes in Saskatchewan. Alternative to the statistical approach used here for definition of site-dependent PI scales, PI intervals related with successional processes could be calibrated with ground samples, whereby negative PI ranges could describe vegetation decline, and positive PI intervals could relate to regrowth, encroachment, or plantation. For application of this method to large areas, ecozones or subregions would constitute natural units, whereby PI scales could be derived in accordance with zone-specific environmental conditions and vegetation structure and composition. Through this work, we have identified some issues that merit further investigation. In particular, the extendibility of the method over large areas poses challenges both in terms of computational effort and parameterization of the methods applied.

CONCLUSIONS

An annual series of Landsat best-available-pixel image composites constitute a valuable source of information for monitoring forest change dynamics at the landscape level over large areas. Pixel locations where observations are missing as a result of limited data availability or atmospheric effects can be filled in or replaced with spatiotemporal interpolation algorithms. The reliability of infill values is dependent on the spatial size and temporal persistence of the data gap. As would be expected, the smaller the temporal and spatial gaps, the more readily an infill value can be interpolated (Table 4). Spatial units with similar vegetation characteristics and change history can be generated via spatiotemporal segmentation of the infilled image composites, supporting the description of landscape dynamics. The Tasseled Cap Angle (TCA) and its temporal derivative, the Process Indicator (PI), are useful tools for characterizing forest state and change processes, describing continuous transformations such as growth and stress, as well as periodic disturbances such as fire and harvest. Knowledge of the nature of a given change process informs the understanding of the causal agents of change. Time-series similarity analysis using dynamic time warping (DTW) and cross-correlation measures provides valuable information about pixel-level composite quality, supporting the identification of anomalous values for replacement. The 3 activities described herein—infill via spatiotemporal interpolation, change detection and characterization via spatiotemporal segmentation and analysis of spectral time-series, and detection and replacement of anomalous pixel values—result in gap-free, cloud-free, large-area proxy value image composites. The change objects and their associated TCA and PI trajectories offer, as shown through the ecologically representative study sites investigated, the ability to characterize both disturbance and postdisturbance processes. The size and duration of disturbance events can be clearly differentiated between one another, as can postdisturbance spectral trends. The spatial detail offered by Landsat data enables capture of management activities on the landscape, and the longevity of the Landsat program provides critical baseline information for ongoing and future monitoring efforts.

ACKNOWLEDGMENTS

The journal editors and reviewers are thanked for their collegial and generous offering of insights that improved this manuscript.

FUNDING

This research was undertaken as part of the "National Terrestrial Ecosystem Monitoring System (NTEMS): Timely and detailed national cross-sector monitoring for Canada" project jointly funded by the Canadian Space Agency (CSA) Government Related Initiatives Program (GRIP) and the Canadian Forest Service (CFS) of Natural Resources Canada.

REFERENCES

Achard, F., and Hansen, M.C. 2013. "Use of Earth observation technology to monitor forests across the globe." In *Global Forest Monitoring from Earth Observation, Chapter 3*. Boca Raton, FL, USA: CRC Press.

Arvidson, T., Goward, S., Gasch, J., and Williams, D. 2006. "Landsat-7 long-term acquisition plan: Development and validation." *Photogrammetric Engineering and Remote Sensing*, Vol. 72: pp. 1137–1146.

Berland, A., Nelson, T., Stenhouse, G., Graham, K., and Crantson, J. 2008. "The impact of landscape disturbance on grizzly bear habitat use in the Foothills Model Forest, Alberta, Canada." *Forest Ecology and Management*, Vol. 256: pp. 1875–1883.

Blaschke, T., Hay, G.J., Kelly, M., Lang, S., Hofmann, P., Addink, E., Feitosa, R.Q., van der Meer, F., van der Werff, H., van Coillie, F., and Tiede, D. 2014. "Geographic object-based image analysis-towards a new paradigm." *ISPRS Journal of Photogrammetry and Remote Sensing*, Vol. 87, pp. 180–191.

Bonsal, B., and Regier, M. 2007. "Historical comparison of the 2001/2002 drought in the Canadian Prairies." *Climate Research*, Vol. 33: pp. 229–242.

Bontemps, S., Bogaert, P., Titeux, N., and Defourny, P. 2008. "An object-based change detection method accounting for temporal dependences in time series with medium to coarse spatial resolution." *Remote Sensing of Environment*, Vol. 112(No. 6): pp. 3181–3191.

Bontemps, S., Langner, A., and Defourny, P. 2012. "Monitoring forest changes in Borneo on a yearly basis by an object-based change detection algorithm using SPOT VEGETATION time series." *International Journal of Remote Sensing*, Vol. 33(No. 15): pp. 4673–4699.

Brandt, J.P., Flannigan, M.D., Maynard, D.G., Thompson, I.D., and Volney, W.J.A. 2013. "An introduction to Canada's boreal zone: ecosystem processes, health, sustainability and environmental issues." *Environmental Reviews*, Vol. 21: pp. 207–226.

Broich, M., Hansen, M.C., Potapov, P., Adusei, B., Lindquist, E., and Stehman, S.V. 2011. "Time-series analysis of multi-resolution optical imagery for quantifying forest cover loss in Sumatra and Kalimantan, Indonesia." *International Journal of Applied Earth Observation and Geoinformation*, Vol. 13: pp. 277–291.

Brooks, E.B., Wynne, R.H., Thomas, V.A., Blinn, C.E., and Coulston, J.W. 2013. "On-the-fly massively multitemporal change detection using statistical quality control charts and Landsat data." *IEEE Transactions on Geosciences and Remote Sensing*, Vol. 52: pp. 3316–3332.

Canadian Forest Service. 2013. *Canadian National Fire Database – Agency Fire Data*. Northern Forestry Centre, Edmonton, AB: Natural Resources Canada/Canadian Forest Service. http://cwfis.cfs.nrcan.gc.ca/en_CA/nfdb. Accessed 11 December 2013.

Castilla, G., Guthrie, R.H., and Hay, G.J. 2009. "The Land-cover Change Mapper (LCM) and its application to timber harvest monitoring in Western Canada." *Photogrammetric Engineering & Remote Sensing*, Vol. 75(No. 8): pp. 941–950.

Chen, G., Hay, G.H., Carvalho, L.M.T., and Wulder, M.A. 2012. "Object-based change detection." *International Journal of Remote Sensing*, Vol. 33(No. 14): pp. 4434–4457.

Chen, J., Zhu, X., Vogelmann J.E., Gao, F., and Jin, S. 2011. "A simple and effective method for filling gaps in Landsat ETM+ SLC-off images." *Remote Sensing of Environment*, Vol. 115: pp. 1053–1064.

Cheng, Q., Shen, H., Zhang, L., Yuan, Q., and Zeng, Ch. 2014. Cloud removal for remotely sensed images by similar pixel replacement guided with a spatio-temporal MRF model. *ISPRS Journal of Photogrammetry and Remote Sensing*, Vol. 92: pp. 54–68.

Coops, N., Wulder, M., and White, J. 2006. "Identifying and describing forest disturbance and spatial pattern: Data selection issues and methodological implications." In *Forest Disturbance and Spatial Pattern: Remote Sensing and GIS Approaches*, edited by M. Wulder, and S. Franklin, Chapter 2. Boca Raton, Florida, USA: Taylor and Francis.

Coppin, P.R., and Bauer, M.E. 1996. "Change detection in forest ecosystems with remote sensing digital imagery." *Remote Sensing Reviews*, Vol. 13: pp. 207–234.

Coppin, P., Jonckherre, I., Nackaerts, K., and Muys, B. 2004. "Digital change detection methods in ecosystem monitoring: a review." *International Journal of Remote Sensing*, Vol. 25: pp. 1565–1596.

Costa, H., Carrão, H., Bacão, F., and Caetano, M. 2014. "Combining per-pixel and object-based classifications for mapping land cover over large areas." *International Journal of Remote Sensing*, Vol. 35(No. 2): pp. 738–753.

Crist, E.P. 1985. "A TM tasseled cap equivalent transformation for reflectance factor data." *Remote Sensing of Environment*, Vol. 17: pp. 301–306.

Desclée, B., Bogaert, P., and Defourny, P. 2006. "Forest change detection by statistical object-based method." *Remote Sensing of Environment*, Vol. 102: pp. 1–11.

Duro, D.C., Coops, N.C., Wulder, M.A., and Han, T. 2007. "Development of a large area biodiversity monitoring system driven by remote sensing." *Progress in Physical Geography*, Vol. 31(No. 3): pp. 1–26.

Duveiller, G., Defourny, P., Desclée, B., and Mayaux, P. 2008. "Deforestation in Central Africa: Estimates at regional, national and landscape levels by advanced processing of systematically distributed Landsat extracts." *Remote Sensing of Environment*, Vol. 112: pp. 1969–1981.

Eastman, J.R., Sangermano, F., Ghimire, B., Zhu, H., Chen, H., Neeti, N., Cai, Y., Machado, E.A., and Crema, S.C. 2009. "Seasonal trend analysis of image time series." *International Journal of Remote Sensing*, Vol. 30(No. 10): pp. 2721–2726.

Ernst, C., Mayaux, P., Verhegghen, A., Bodart, C., Christophe, M., and Defourny, P. 2013. "National forest cover change in Congo Basin: deforestation, reforestation, degradation and regeneration for the years 1990, 2000 and 2005." *Global Change Biology*, Vol. 19: pp. 1173–1187.

Ecological Stratification Working Group, 1995. *A National Ecological Framework for Canada. Agriculture and Agri-Food Canada, Research Branch*. Ottawa/Hull: Centre for Land and Biological Resources Research and Environment Canada, State of the Environment Directorate, Ecozone Analysis Branch.

Franklin, J.F., Spies, T.A., Van Pelt, R., Carey, A.B., Thornburgh, D.A., Rae Berg, D., Lindenmayer, D.B., Harmon, M.E., Keeton, W.S., Shaw, D.C., Bible, K., and Chen, J. 2002. "Disturbances and structural development of natural forest ecosystems with silvicultural implications, using Douglas-fir forests as an example." *Forest Ecology and Management*, Vol. 155: pp. 399–423.

Frazier, R.J., Coops, N.C., Wulder, M.A., and Kennedy, R. 2014. "Characterization of aboveground biomass in an unmanaged boreal forest using Landsat temporal segmentation metrics." *ISPRS Journal of Photogrammetry and Remote Sensing*, Vol. 92: pp. 137–146.

Frolking, S., Palace, M.W., Clark, D.B., Chambers, J.Q., and Shugart, H.H. 2009. "Forest disturbance and recovery: a general review in the context of spaceborne remote sensing of impacts on aboveground biomass and canopy structure." *Journal of Geophysical Research*, Vol. 114: pp. 1–27.

García, D., 2010. "Robust smoothing of gridded data in one and higher dimensions with missing values." *Computational Statistics and Data Analysis*, Vol. 54: pp. 1167–1178.

Gillanders, S.N., Coops, N.C., Wulder, M.A., and Goodwin, N.R. 2008. "Application of Landsat satellite imagery to monitor land-cover changes at the Athabasca Oil Sands, Alberta, Canada." *Canadian Geographer*, Vol. 52(No. 4): pp. 466–485.

Giorgino, T. 2009. "Computing and visualizing dynamic time warping alignments in R: the dtw package." *Journal of Statistical Software*, Vol. 31(No. 7): pp. 1–24.

Gómez, C., White, J.C., and Wulder, M.A. 2011. "Characterizing the state and processes of change in a dynamic forest environment using hierarchical spatio-temporal segmentation." *Remote Sensing of Environment*, Vol. 115: pp. 1665–1679.

Gómez, C., White, J.C., Wulder, M.A., and Alejandro, P. 2014. "Historical biomass and carbon dynamics modelled with Landsat spectral trajectories." *ISPRS Journal of Photogrammetry and Remote Sensing*, Vol. 93: pp. 14–28.

Gómez, C., Wulder, M.A., White, J.C., Montes, F., and Delgado, J.A. 2012. "Characterizing 25 years of change in the area, distribution, and carbon stock of Mediterranean pines in Central Spain." *International Journal of Remote Sensing*, Vol. 33(No. 17): pp. 5546–5573.

Gong, P., and Xu, B. 2003. "Remote sensing of forests over time: change types, methods, and opportunities." In *Remote Sensing of Forest Environments: Concepts and Case Studies*, edited by M.A. Wulder and S.E. Franklin, pp. 301–333. Norwell, MA: Kluwer Academic.

Goodwin, N.R., and Collett, L.J. 2014. "Development of an automated method for mapping fire history captured in Landsat TM and ETM+ time series across Queensland, Australia." *Remote Sensing of Environment*, Vol. 148: pp. 206–221.

Goodwin, N.R., Coops, N.C., Wulder, M.A., Gillanders, S., Schroeder, T.A., and Nelson, T. 2008. "Estimation of insect infestation dynamics using temporal series of Landsat data." *Remote Sensing of Environment*, Vol. 112: pp. 3680–3689.

Griffiths, P., Kuemmerle, T., Baumann, M., Radeloff, V.C., Abrudan, I.V., Lieskovsky, J., Munteanu, C., Ostapowicz, K., and Hostert, P. 2013. "Forest disturbances, forest recovery, and changes in forest types across the Carpathian ecoregion from 1985 to 2010 based on Landsat image composites." *Remote Sensing of Environment*, Vol. 151: pp. 72–88.

Griffiths, P., Van der Linden, S., Kuemmerle, T., and Hostert, P. 2013. "A pixel-based Landsat compositing algorithm for large area land cover mapping." *IEEE Journal of Selected Topics in Applied Earth Observations and Remote Sensing*, Vol. 6(No. 5): 2088–2101.

Hais, M., Jonášová, M., Langhammer, J., and Kučera, T. 2009. "Comparison of two types of forest disturbance using multitemporal Landsat TM/ETM+ imagery and field vegetation data." *Remote Sensing of Environment*, Vol. 113: pp. 835–845.

Hall, O., and Hay, G.J. 2003. "A multiscale object-specific approach to digital change detection." *International Journal of Applied Earth Observation and Geoinformation*, Vol. 4: pp. 311–327.

Hansen, M.C., and Loveland, T.R. 2012. "A review of large area monitoring of land cover change using Landsat data." *Remote Sensing of Environment*, Vol. 122: pp. 66–74.

Hermosilla, T., Wulder, M.A., White, J.C., Coops, N.C., and Hobart, G.W. 2015. "An integrated Landsat time series protocol for change detection and generation of annual gap-free surface reflectance composites." *Remote Sensing of Environment*, Vol. 158: pp. 220–234.

Hofmann, P., and Blaschke, T. 2012. "Object based change detection using temporal linkages." Paper presented at Proceedings of the 4th GEOBIA, Rio de Janeiro, Brazil, May 7–9.

Houghton, R.A., House, J.I., Pongratz, J., van del Werf, G.R., DeFries, R.S., Hansen, M.C., LeQuere, C., and Ramankutty, N. 2012. "Carbon emissions from land use and land-cover change." *Biogeosciences*, Vol. 9: pp. 5125–5142.

Huang, Ch., Goward, S.N., Masek, J.G., Gao, F., Vermote, E.F., Thomas, N., Schleeweis, K., Kennedy, R.E., Zhu, Z., Eidenshink, J.C., and Townshend, J.R.G. 2009. "Development of time series stacks of Landsat images for reconstructing forest disturbance history." *International Journal of Digital Earth*, Vol. 1: pp. 1–25.

Huang, Ch., Goward, S.N., Masek, J.G., Thomas, N., Zhu, Zh., and Vogelmann, J.E. 2010. "An automated approach for reconstructing recent forest disturbance history using dense Landsat time series stacks." *Remote Sensing of Environment*, Vol. 114: pp. 183–198.

Huang, Ch., Goward, S.N., Schleeweis, K., Thomas, N., Masek, J.G., and Zhu, Z. 2009. "Dynamics of national forests assessed using Landsat record: Case studies in eastern United States." *Remote Sensing of Environment*, Vol. 113: pp. 1430–1442.

Hussain, M., Chen, D., Cheng, A., Wei, H., and Stanley, D. 2013. "Change detection from remotely sensed images: from pixel-based to object-based approaches." *ISPRS Journal of Photogrammetry and Remote Sensing*, Vol. 80: pp. 91–106.

Jensen, J.R., 2005. *Introductory Digital Image Processing. A Remote Sensing Perspective*. Upper Saddle River, NJ, USA: Prentice Hall.

Jin, S., and Sader, S.A. 2005. "Comparison of time series tasseled cap wetness and the normalized difference moisture index in detecting forest disturbances." *Remote Sensing of Environment*, Vol. 94, pp. 364–372.

Johansen, K., Arroyo, L.A., Phinn, S., and Witte, C. 2010. "Comparison of geo-object based and pixel-based change detection of riparian environments using high spatial resolution multi-spectral imagery." *Photogrammetric Engineering & Remote Sensing*, Vol. 76: pp. 123–136.

Kennedy, R.E., Andréfouët, S., Gómez, C., Griffiths, P., Hais, M., Healey, S., Helmer, E.H., Hostert, P., Lyons, M., Meigs, G.W., Pflugmacher, D., Phinn, S., Powell, S., Scarth, P.F., Sen, S., Schroeder, T.A., Schneider, A-M., Sonnenschein, R., Vogelmann, J.E., Wulder, M.A., and Zhu, Z. 2014. "Bringing an ecological view of change to Landsat-based remote sensing." *Frontiers in Ecology and Environment*, Vol. 12(No. 6): pp. 339–346.

Kennedy, R.E., Cohen, W.B., and Schroeder, T.A. 2007. "Trajectory-based change detection for automated characterization of forest disturbance dynamics." *Remote Sensing of Environment*, Vol. 110: pp. 370–386.

Kennedy, R.E., Zhiqiang, Y., and Cohen, W. 2010. "Detecting trends in forest disturbance and recovery using yearly Landsat time series: 1. LandTrendr – Temporal segmentation algorithms." *Remote Sensing of Environment*, Vol. 114: pp. 2897–2910.

Kennedy, R.E., Zhiqiang, Y., Cohen, W.B., Pfaff, E., Braaten, J., and Nelson, P. 2012. "Spatial and temporal patterns of forest disturbance and regrowth within the area of the Northwest Forest Plan." *Remote Sensing of Environment*, Vol. 122: pp. 117–133.

Kindu, M., Schneider, T., Teketay, D., and Knoke, T. 2013. "Land use/land cover change analysis using object-based classification approach in Munessa-Shashemene landscape of the Ethiopian highlands." *Remote Sensing*, Vol. 5: pp. 2411–2435.

Kurz, W.A., Shaw, C.H., Boisvenue, C., Stinson, G., Metsaranta, J., Leckie, D., Dyk, A., Smyth, C., and Neilson, E.T. 2013. "Carbon in Canada's forest–a synthesis." *Environmental Reviews*, Vol. 21: pp. 260–292.

Kurz, W.A., Stinson, G., Rampley, G.J., Dymond, C.C., and Neilson, E.T. 2008. "Risk of natural disturbances makes future contribution of Canada's forests to the global carbon cycle highly uncertain." *Proceedings of the National Academy of Sciences of the United States of America*, Vol. 105(No. 5): pp. 1551–1555.

LeQuéré, C., Andres, R.J., Boden, T., Conway, T., Houghton, R.A., House, J.I., Marland, G., Peters, G.P., van der Werf, G., Ahlstrom, A., Andrew, R.M., Bopp, L., Canadell, J.G., Ciais, P., Doney, S.C., Enright, C., Friedlingstein, P., Huntingford, C., Jain, A.K., Jourdain,

C., Kato, E., Keeling, R.F., Goldewijk, K.K., Levis, S., Levy, P., Lomas, M., Poulter, B., Raupach, M.R., Schwinger, J., Sitch, S., Stocker, B.D., Viovy, N., Zaehle, S., and Zeng, N. 2012. "The global carbon budget 1959–2011." *Earth Systems Science Data Discussion*, Vol. 5: pp. 1107–1157.

LeQuéré, C., Raupach, M.R., Canadell, J.G., Marland, G., Bopp, L., Ciais, Ph., Conway, T.J., Doney, S.C., Feely, R.A., Foster, P., Friedlingstein, P., Gurney, K., Houghton, R.A., House, J.I., Huntingford, Ch., Levy, P.E., Lomas, M.R., Majkut, J., Metzl, N., Ometto, J.P., Peters, G.P., Prentice, I.C., Randerson, J.T., Running, S.W., Sarmiento, J.L., Schuster, U., Sitch, S., Takahashi, T., Viovy, N., van der Werf, G.R., and Woodward, F.I. 2009. "Trends in the sources and carbon sinks of carbon dioxide." *Nature Geoscience*, Vol. 2: pp. 831–836.

Li, X., Yeh, A.G., Qian, J., Ai, B., and Qi, Z. 2009. "A matching algorithm for detecting land use changes using case-based reasoning." *Photogrammetric Engineering & Remote Sensing*, Vol. 75: pp. 1319–1332.

Linke, J., and McDermid, G.J. 2012. "Monitoring landscape change in multi-use west-central Alberta, Canada using the disturbance-inventory framework." *Remote Sensing of Environment*, Vol. 125: pp. 112–124.

Linke, J., McDermid, G.J., Laskin, D.N., McLane, A.J., Pape, A., Cranston, J., Hall-Beyer, M., and Franklin, S.E. 2009. "A disturbance-inventory framework for flexible and reliable landscape monitoring." *Photogrammetric Engineering & Remote Sensing*, Vol. 75(No. 8): pp. 981–995.

Long, J.N., 2009. "Emulating natural disturbance regimes as a basis for forest management: A North American view." *Forest Ecology and Management*, Vol. 257: pp. 1868–1873.

Lu, D., Mausel, P., Bronzdizio, E., and Moran, E. 2004. "Change detection techniques." *International Journal of Remote Sensing*, Vol. 25: pp. 2365–2407.

Lunetta, R.S., Johnson, D.M., Lyon, J.G., and Crotwell, J. 2004. "Impacts of imagery temporal frequency on land-cover change detection monitoring." *Remote Sensing of Environment*, Vol. 89: pp. 444–454.

Malila, W. 1980. "Change vector analysis: an approach for detecting forest changes with Landsat." *Proceedings of the 6th Annual Symposium on Machine Processing of Remotely Sensed Data*, pp. 326–335. West Lafayette, IN: Purdue University Press.

Masek, J.G., Huang, Ch., Wolfe, R., Cohen, W., Hall, F., Kutler, J., and Nelson, P. 2008. "North American forest disturbance mapped from a decadal Landsat record." *Remote Sensing of Environment*, Vol. 112: pp. 2914–2926.

Masek, J.G., Vermote, E.F., Saleous, N.E., Wolfe, R., Hall, F.G., Huemmrich, K.F., Gao, F., Kutler, J., and Lim, T.K. 2006. "A Landsat surface-reflectance dataset for North America, 1990–2000." *IEEE Geoscience and Remote Sensing Letters*, Vol. 3(No. 1): pp. 68–72.

Maxwell, S.K. 2004. "Filling landsat ETM+ SLC-off gaps using a segmentation model approach." *Photogrammetric Engineering and Remote Sensing*, Vol. 70: pp. 1109–1111.

Maxwell, S.K., Schmidt, G.L., and Storey, J.C. 2007. "A multi-scale segmentation approach to filling gaps in Landsat ETM+ SLC-off images." *International Journal of Remote Sensing*, Vol. 28: pp. 5339–5356.

McDermid, G.J., Linke, J., Pape, A.D., Laskin, D.N., McLane, A.J., and Franklin, S.E. 2008. "Object-based approaches to change analysis and thematic map update: challenges and limitations." *Canadian Journal of Remote Sensing*, Vol. 34(No. 5): pp. 462–466.

Nijland, W., Addink, E.A., de Jong, S.M., and van der Meer, F. 2010. "Detection of ecosystem functioning using object-based time-series analysis." Paper presented at GEOBIA 2010-Geographic Object-Based Image Analysis, University of Ghent, Ghent, Belgium, 29 June–2 July 2010. http://dfwm.ugent.be/geobia/proceedings/papers%20proceedings/Nijland_182_Detection%20of%20ecosystem%20functioning%20using%20object-based%20time-series%20analysis.pdf. Accessed December 15, 2013.

Oliver, C.D., and Larson, B.C. 1996. *Forest Stand Dynamics. Updated edn*. New York, NY: Wiley.

Olofsson, P., Foody, G.M., Herold, M., Stehman, S.V., Woodcock, C.E., and Wulder, M.A. 2014. "Good practices for estimating area and assessing accuracy of land change." *Remote Sensing of Environment*, Vol. 148: pp. 42–57.

Parisien, M.A., Hirsch, K.G., Lavoie, S.G., Todd, J.B., and Kafka, V.G. 2004. *Saskatchewan Fire Regime Analysis*, Inf. Rep. NOR-X-39. Northern Forest Center, Edmonton, AB, Canada: Natural Resources Canada/Canadian Forest Service.

Parmentier, B., and Eastman, J.R. 2014. "Land transitions from multivariate time series: using seasonal trend analysis and segmentation to detect land-cover changes." *International Journal of Remote Sensing*, Vol. 35(No. 2): pp. 671–692.

Pflugmacher, D.L., Cohen, W.B., and Kennedy, R.E. 2012. "Using Landsat-derived disturbance history (1972–2010) to predict current forest structure." *Remote Sensing of Environment*, Vol. 122: pp. 146–165.

Potapov, P., Turubanova, S., and Hansen, M.C. 2011. "Regional-scale boreal forest cover and change mapping using Landsat data composites for European Russia." *Remote Sensing of Environment*, Vol. 115: pp. 548–561.

Potapov, P.V., Turubanova, S.A., Hansen, M.C., Adusei, B., Broich, M., Altstatt, A., Mane, L., and Justice, C.O. 2012. "Quantifying forest cover loss in loss in Democratic Republic of the Congo, 2000–2010, with Landsat ETM + data." *Remote Sensing of Environment*, Vol. 122: pp. 106–116.

Powell, S.L., Cohen, W.B., Healey, S.P., Kennedy, R.E., Moisen, G.G, Pierce, K.B., and Ohmann, J.L. 2010. "Quantification of live above-ground biomass dynamics with Landsat time-series and field inventory data: a comparison of empirical modeling approaches." *Remote Sensing of Environment*, Vol. 114: pp. 1053–1068.

Power, K., and Gillis, M. 2006. *Canada's Forest Inventory 2001*. Natural Resources Canada/Canadian Forest Service.

Pringle, M.J., Schmidt, M., and Muir, J.S. 2009. "Geostatistical interpolation of SLC-off Landsat ETM plus images." *ISPRS Journal of Photogrammetry and Remote Sensing*, Vol. 64: pp. 654–664.

Roy, D.P., Ju, J., Kline, K., Scaramuzza, P.L., Kovalskyy, V., Hansen, M., Loveland, T.R., Vermote, E., and Zhang, Ch. 2010. "Web-enabled Landsat data (WELD): Landsat ETM+ composited mosaics of the conterminous United States." *Remote Sensing of Environment*, Vol. 114: pp. 35–49.

Roy, D.P., Ju, J., Lewis, P., Schaaf, C., Gao, F., Hansen, M., and Lindquist, E. 2008. "Multi-temporal MODIS-Landsat data fusion for relative radiometric normalization, gap filling, and prediction of Landsat data." *Remote Sensing of Environment*, Vol. 112: pp. 3112–3130.

Roy, D.P., Ju, J., Mbow, Ch., Frost, Ph., and Loveland, T. 2010. "Accessing free Landsat data via the Internet: Africa's challenge." *Remote Sensing Letters*, Vol. 1(No. 2): pp. 111–117.

Roy, D., Wulder, M.A., Loveland, T.R., Woodcock, C.E., Allen, R.G., Anderson, M.C., Helder, D., Irons, J.R., Johnson, D.M., Kennedy, R., Scambos, T.A., Schaaf, C.B., Schott, J.R., Sheng, Y., Vermote, E.F., Belward, A.S., Bindschadler, R., Cohen, W.B., Gao, F., Hipple, J.D., Hostert, P., Huntington, J., Justice, C.O., Kilic, A., Kovalskyy, V., Lee, Z.P. Lymburner, L., Masek, J.G., McCorkel, J., Shuai, Y., Trezza, R., Vogelmann, J., Wynne, R.H., and Zhu, Z. 2014. "Landsat–8: science and product vision for terrestrial global change research." *Remote Sensing of Environment*, Vol. 145: pp. 154–172.

Saksa, T., Uuttera, J., Kolström, T., Lehikoinen, M., Pekkarinen, A., and Sarvi, V. 2003. "Clear-cut detection in boreal forest aided by remote sensing." *Scandinavian Journal of Forest Research*, Vol. 18: pp. 537–546.

Saskatchewan Ministry of Environment. 2012. *Report on Saskatchewan Forests*. http://www.environment.gov.sk.ca/adx/aspx/adxGetMedia.aspx?DocID=f7181d1f-fd4b-4ab9-8720-07cceb877437&MediaID=1648e1a4-01f4-4936-a92b-3e2880a39b55&Filename=2012±Report±on±Saskatchewan±Forests.pdf&l=English. Accessed February 25, 2014.

Schmidt, G., Jenkerson, C., Masek, J., Vermote, E., and Gao, F. 2013. *Landsat Ecosystem Disturbance Adaptive Processing System (LEDAPS) Algorithm Description*. Open-File Report 2013–1057. Washington, DC: US Department of the Interior, USGS.

Schroeder, T.A., Wulder, M.A., Healey, S.P., and Moisen, G.G. 2011. "Mapping wildfire and clearcut harvest disturbances in boreal forests with Landsat time series data." *Remote Sensing of Environment*, Vol. 115: pp. 1421–1433.

Singh, A. 1989. "Digital change detection techniques using remotely-sensed data." *International Journal of Remote Sensing*, Vol. 10: pp. 989–1003.

Taylor, A.R., Seedre, M., Brassard, B.W., and Chen, H.Y.H. 2014. "Decline in net ecosystem productivity following canopy transition to late-succession forests." *Ecosystems*, doi:10.1007/s10021-014-9759-3.

Tormene, P., Giorgino, T., Quaglini, S., and Stefanelli, M. 2009. "Matching incomplete time series with dynamic time warping: an algorithm and an application to post-stroke rehabilitation." *Artificial Intelligence in Medicine*, Vol. 45: pp. 11–34.

USGS. 2004. "Phase 2 gap-fill algorithm: SLC-off gap-filled products gap-fill algorithm methodology." Accessed March 30, 2015, landsat.usgs.gov/documents/L7SLCGapFilledMethod.pdf

Verhegghen, A., Ernst, C., Defourny, P., and Beuchle, R. 2010. "Automated land cover mapping and independent change detection in tropical forest using multi-temporal high resolution data set." *The International Archives of the Photogrammetry, Remote Sensing and Spatial Information Sciences*, Vol. XXXVIII–4/C7.

Vogelmann, J.E., Tolk, B., and Zhu, Z. 2009. "Monitoring forest changes in the southwestern United States using multitemporal Landsat data." *Remote Sensing of Environment*, Vol. 113: pp. 1739–1748.

Walter, V., 2004. "Object-based classification of remote sensing data for change detection." *ISPRS Journal of Photogrammetry and Remote Sensing*, Vol. 58: pp. 225–238.

Wang, G., García, D., Liu, Y., de Jeu, R., and Dolman, A.J. 2012. "A three-dimensional gap filling method for large geophysical datasets: Application to global satellite soil moisture observations." *Environmental Modelling and Software*, Vol. 30: pp. 139–142.

White, J.C., and Wulder, M.A. 2013. "The Landsat observation record of Canada: 1972–2012." *Canadian Journal of Remote Sensing*, Vol. 39(No. 6): pp. 455–467.

White, J.C., Wulder, M.A., Gómez, C., and Stenhouse, G. 2011. "A history of habitat dynamics: characterizing 35 years of stand replacing disturbance." *Canadian Journal of Remote Sensing*, Vol. 37(No. 2): pp. 234–251.

White, J.C., Wulder, M.A., Hobart, G.W., Luther, J.E., Hermosilla, T., Griffiths, P., Coops, N.C., Hall, R.J., Hostert, P., Dyk, A., and Guindon, L. 2014. "Pixel-based image compositing for large-area dense time series applications and science." *Canadian Journal of Remote Sensing*, Vol. 40(No. 3): pp. 192–212.

Whittaker, E.T. 1923. "On a new method of graduation." *Proceedings of the Edinburgh Mathematical Society*, Vol. 41: pp. 62–75.

Wulder, M.A., and Coops, N.C. 2014. "Make Earth observations open access." *Nature*, Vol. 513(No. 7516): pp. 30–31.

Wulder, M.A., Masek, J.G., Cohen, W.B., Loveland, T.R., and Woodcock, C.E. 2012. "Opening the archive: How free data has enabled the science and monitoring promise of Landsat." *Remote Sensing of Environment*, Vol. 122: pp. 2–10.

Wulder, M.A., and Seemann, D. 2003. "Forest inventory height update through the integration of LiDAR data with segmented Landsat imagery." *Canadian Journal of Remote Sensing*, Vol. 29(No.5): pp. 536–543.

Wulder, M.A., White, J.C., Cranny, M., Hall, R.J., Luther, J.E., Beaudoin, A., Goodenough, D.G., and Dechka, J.A. 2008. "Monitoring Canada's forests. Part 1: completion of the EOSD land cover project." *Canadian Journal of Remote Sensing*, Vol. 34(No. 6): pp. 549–562.

Wulder, M.A., White, J.C., and Coops, N.C. 2011. "Fragmentation regimes of Canada's forests." *The Canadian Geographer*, Vol. 55(No. 3): pp. 288–300.

Wulder, M.A., White, J.C., Goward, S.M., Masek, J.G., Irons, J.R., Herold, M., Cohen, W.B., Loveland, Th.R., and Woodcock, C.E. 2008. "Landsat continuity: issues and opportunities for land cover monitoring." *Remote Sensing of Environment*, Vol. 112: pp. 955–969.

Xian, G., Homer, C., and Fry, J. 2009. "Updating the 2001 National Land Cover Database land cover classification to 2006 by using Landsat imagery change detection methods." *Remote Sensing of Environment*, Vol. 113: pp. 1133–1147.

Zeng, C., Shen, H., and Zhang, L. 2013. "Recovering missing pixels for Landsat ETM+ SLC-off imagery using multi-temporal regression analysis and a regularization method." *Remote Sensing of Environment*, Vol. 131: pp. 182–194.

Zhang, C., Li, W., and Travis, D. 2007. "Gaps-fill of SLC-off Landsat ETM plus satellite image using a geostatistical approach." *International Journal of Remote Sensing*, Vol. 28: pp. 5103–5122.

Zhu, X., Liu, D., and Chen, J. 2012. "A new geostatistical approach for filling gaps in Landsat ETM+ SLC-off images." *Remote Sensing of Environment*, Vol. 124: pp. 49–60.

Zhu, Z., Wang, Sh., and Woodcock, C.E. 2015. "Improvement and expansion of the Fmask algorithm: cloud, cloud shadow, and snow detection for Landsats 4–7, 8, and Sentinel 2 images." *Remote Sensing of Environment*, Vol. 159: pp. 269–277.

Zhu, Z., and Woodcock, C.E. 2012. "Object-based cloud and cloud shadow detection in Landsat imagery." *Remote Sensing of Environment*, Vol. 118: pp. 83–94.